AD A101349

AFWAL-TR-80-4172

FATIGUE BEHAVIOR OF COMPOSITE LAMINATES

H. Thomas Hahn
D. G. Hwang

Washington University
Materials Research Laboratory
St. Louis, MO   63130

November 1980

TECHNICAL REPORT AFWAL-TR-80-4172

Final Report for Period 1 September 1979 - 29 August 1980

Approved for public release; distribution unlimited.

JUL 1 4 1981

A

81 7 13 017

REPORT DOCUMENTATION PAGE	READ INSTRUCTIONS BEFORE COMPLETING FORM

1. REPORT NUMBER	2. GOVT ACCESSION NO.	3. RECIPIENT'S CATALOG NUMBER
AFWAL-TR-80-4172	AD-A101349	

4. TITLE (and Subtitle)	5. TYPE OF REPORT & PERIOD COVERED
Fatigue Behavior of Composite Laminates	Final Technical 1 Sept. 1979-29 Aug. 1980.
	6. PERFORMING ORG. REPORT NUMBER

7. AUTHOR(s)	8. CONTRACT OR GRANT NUMBER(s)
H. Thomas Hahn D. G. Hwang	F33615-77-C-5053

9. PERFORMING ORGANIZATION NAME AND ADDRESS	10. PROGRAM ELEMENT, PROJECT, TASK AREA & WORK UNIT NUMBERS
Washington University Materials Research Laboratory St. Louis, MO 63130	24190314 (formerly 2307P107)

11. CONTROLLING OFFICE NAME AND ADDRESS	12. REPORT DATE
Air Force Wright Aeronautical Laboratories (MLBM) Air Force Systems Command Wright-Patterson AFB, OH 45433	November 1980
	13. NUMBER OF PAGES
	94

14. MONITORING AGENCY NAME & ADDRESS(if different from Controlling Office)	15. SECURITY CLASS. (of this report)
	Unclassified
	15a. DECLASSIFICATION/DOWNGRADING SCHEDULE

16. DISTRIBUTION STATEMENT (of this Report)

Approved for public release; distribution unlimited.

17. DISTRIBUTION STATEMENT (of the abstract entered in Block 20, if different from Report)

18. SUPPLEMENTARY NOTES

19. KEY WORDS (Continue on reverse side if necessary and identify by block number)

Graphite/Epoxy Laminates, Static Strength, Fatigue, Scatter, Statistical Distribution, Proof Test, Failure Mode.

20. ABSTRACT (Continue on reverse side if necessary and identify by block number)

The main objective of this program during the final reporting period was to investigate the fatigue behavior of a $[0_2/90/\pm45]_s$ AS/3501-5A Gr/Ep laminate through proof testing. The primary emphasis was on the delineation of the effect of proof test on the residual strength and life, the establishment of strength-life relations, and the identification of sources of scatter in strength and life. The test program consisted of static tests, — — ....

(continued)

DD FORM 1473 1 JAN 73 EDITION OF 1 NOV 65 IS OBSOLETE

20. (continued)

tension-tension fatigue tests preceded by proof tests, and examinations of failure characteristics. Major findings can be summarized as follows:
(1) Proof tests have little effect on the residual strength and life;
(2) A relation exists between strength and life such that a statically stronger specimen has a longer life; (3) A minimum life can be assured by a proof test; (4) A higher modulus is an indication of a higher strength and longer life; (5) What distinguishes a typical static failure mode from a typical fatigue failure mode is the lack of delamination in the former;
(6) At a moderate fatigue stress, the failure mode changes from a static failure mode to a typical fatigue failure mode around 20,000 cycles; and
(7) A delamination surface consists of shiny and dull areas. The shiny area has bare fibers whereas the dull area only has fiber traces in the epoxy.

FOREWORD

This is the final report on the results of a program entitled

"Fatigue Behavior of Composite Laminates" completed at Washington

University in St. Louis under Air Force Contract F33615-77-C-5053.

The work was performed under Project 2419, "Nonmetallic Structural

Materials," Task No. 241903, "Composite Materials and Mechanics

Technology." The Air Force Project Engineer directing the program

was Dr. S. W. Tsai of the Mechanics and Surface Interactions Branch,

Nonmetallic Materials Division, Materials Laboratory, Air Force Wright

Aeronautical Laboratories, Wright-Patterson AFB, Ohio. For the period

of 2 May 1977 to 31 August 1979, Dr. J. L. Kardos and Mr. N. Q. Nguyen

were the principal investigator and co-principal investigator,

respectively. For the present reporting period of 1 September 1979

- August 1980, Dr. H. T. Hahn was the principal investigator. He

was assisted by Mr. D. G. Hwang.

The authors gratefully acknowledge the support of the Materials

Laboratory for this program. They also wish to express their appreciation

to Mr. B. Sunier for helping with the testing and to Ms. J. Kirby for

typing the manuscript.

iii

TABLE OF CONTENTS

LIST OF ILLUSTRATIONS

LIST OF ILLUSTRATIONS

LIST OF ILLUSTRATIONS

LIST OF TABLES

SECTION I

INTRODUCTION

For most materials the failure properties such as strength and lifetime exhibit more scatter than other properties. The reason is known to be that these failure properties are sensitive to local defects which vary significantly from element to element even though all the elements are made of the same material under the same manufacturing condition. Within the general framework of reliability, such elements are called similar [1].

Composite materials are no exception. Interestingly, however, several investigations [2-7] have shown a possible existence of a relationship between static strength and life. The relationship is such that, among the similar elements, a stronger element also has a longer life.

The strength-life relationship, once proven, will no doubt be very helpful in proof testing of composite structures because one can then provide a certain degree of assurance as not only to the inherent strength of the structures but also to the expected lifetime. Aside from these practical benefits, an investigation on such relationship will lead to a better understanding of the fatigue failure mechanisms and of the variability of fatigue life in composites.

1

The main objective of the present program was thus to investigate
the fatigue behavior of a graphite/epoxy laminate through proof
testing. In particular, the effect of proof test on both the sub-
sequent strength and the subsequent life was to be delineated, and the
appropriate strength-life relationships were to be established. Also
to be identified were the sources of the scatter in fatigue life.

In general terms, proof testing is a procedure to assess the
structural integrity of a structure by loading it to a predetermined
level, called the proof stress. One obvious application of proof
testing is to ascertain a lower bound strength of a specimen: if the
specimen survives the proof test, its strength is definitely larger
than the proof stress applied. The corresponding lower bound life
under a given load history is then the least of the lives of those
specimens that survive the proof test. If there is a unique relation-
ship between strength and life, then this lower bound life can be
predicted.

In multidirectional composite laminates, the final failure under
a tensile loading is invariably preceded by failures of weaker plies
and, depending on the stacking sequence, delamination [8-14]. If the
proof stress is higher than the first ply-failure stress, some of the
weaker plies will fail during the proof test. The question is then
what is the effect of the damage induced by proof test on the
subsequent mechanical properties, in particular, strength and life.

The effect of proof test on the subsequent strength was found to
be negligible for a unidirectional Gr/Ep laminate in Reference [6].

2

Such conclusion is certainly related to the so-called Kaiser effect
in acoustic emission behavior of composites. That is, the detectable
acoustic emission activities during reloading of a composite are
negligible until the maximum previously applied stress is exceeded
[15-17]. Since the acoustic emission is an indication of damage
occurring, the Kaiser effect can be taken as a manifestation of the
extent of damage depending only on the maximum previously applied
stress.

In multidirectional laminates much of the subcritical damage occurs
in the matrix and interface whose properties are time-dependent.
Therefore, acoustic emission can start at a stress lower than the
maximum previously applied stress, the difference increasing with the
latter. Since this is an indication of an additional damage, the
corresponding strength can be different from the initial one. Thus,
it still remains to be seen how high a proof stress can be without
affecting the subsequent strength.

Of much more importance is the effect of proof test-induced
damage on the subsequent life under a given load history. As an
example, consider a constant-amplitude fatigue. If the proof stress
is higher than the fatigue stress, the resulting damage will be larger
than would be after a first cycle of fatigue without the proof test.

The larger subcritical damage does not necessarily lead to a
shorter fatigue life. To illustrate this point, consider the damage to
be the cracks in the 90-deg plies of a $[0/90]_s$ laminate. After a
proof test above the fatigue stress, there will be more cracks in the

90-deg plies than after a first cycle of fatigue without the proof test. When there are more cracks, the average stress in the 90-deg plies will be lower and hence, it will take longer for these plies to fail again. However, without the proof test the average stress in the 90-deg plies will be higher because there is less stress relief by cracking of the plies. Therefore, it is possible that without the proof test more cracks can be formed in time in the 90-deg plies.

Turning now to the stress concentrations on the 0-deg plies at cracks in the 90-deg plies, we observe that after a proof test there are more stress raisers, but of lower magnitude. At present, it is not clear whether or not many stress raisers of lower magnitude are more deleterious than a few stress raisers of higher magnitude.

In this report we attempt to answer some of the questions raised in the foregoing discussions by analyzing the pertinent experimental data. In particular, we delineate the effects of proof test on the subsequent strength and life. Then, we investigate strength-life relationships at two different fatigue stress levels. We explore the possibility of using the initial modulus as a measure of structural integrity, and establish a correlation between life and final failure mode. Also, the effects of gripping on the strength and life are looked into. Finally, some of the failure surfaces are examined through the Scanning Electron Microscope (SEM).

4

SECTION II

EXPERIMENTAL PROCEDURE

1. MATERIAL

The composite used in the program was $[0_2/90/\pm45]_s$ AS/3501-5A laminate. The standard cure cycle with the exception of the post cure was employed to fabricate 610 mm x 610 mm plates by the University of Dayton Research Institute. The average fiber volume content was 66%. Further details on the physical properties of the laminates can be found in Reference [18]. Panels 10 through 12 were fabricated in 1977 whereas panel A was additionally fabricated in 1979.
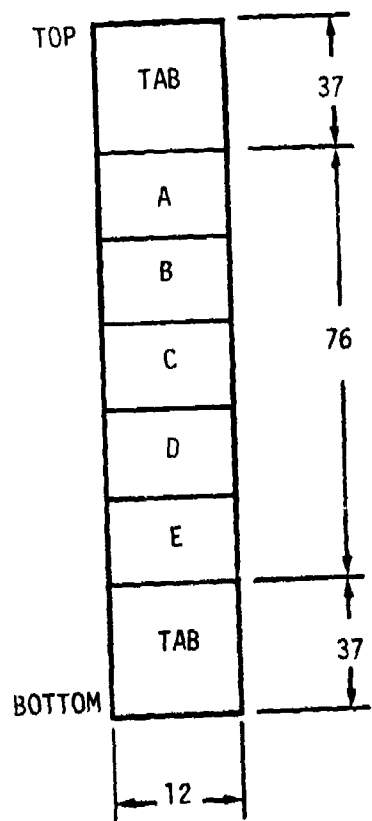
2. SPECIMEN GEOMETRY

Specimens were 12 mm wide and 150 mm long with 76 mm of gage section. Woven glass/epoxy sheets 1.6 mm thick were used as end tabs. Each specimen was divided into 5 zones of equal length to identify failure location, as shown in Figure 1. Zone E was next to the moving grip.

A few specimens were made twice as wide but of the same length. These specimens were used to study the effect of width on strength.

3. TEST METHODS

All mechanical tests were done on an MTS machine. The loading rate in static and proof tests was 100 N/s. Fatigue tests were performed at the stress ratio R of 0.1 and the frequency f of 5 Hz. A sinusoidal wave form was used.

5

```
          TOP  ┌─────────┐  ▲
               │         │  │
               │   TAB   │  │  37
               │         │  │
               ├─────────┤  ▼
               │    A    │
               ├─────────┤
               │    B    │
               ├─────────┤     ▲
               │    C    │     │  76
               ├─────────┤     │
               │    D    │
               ├─────────┤
               │    E    │
               ├─────────┤  ▲
               │         │  │
               │   TAB   │  │  37
        BOTTOM └─────────┘  ▼

                 ├── 12 ──┤
```

DIMENSIONS IN mm

Figure 1. Identification of Failure Zones.

6

In proof testing specimens were loaded to a predetermined stress level and then unloaded. The proof stress levels chosen were 0.87 $\overline{X}$ and 0.95 $\overline{X}$ where $\overline{X}$ is the average static strength. In fatigue, an additional proof stress was chosen: the fatigue stress itself.

During each proof test the axial strain was measured using an extensometer. After a proof test, specimens were tested either for residual strength or in fatigue until failure or 10^6 cycles whichever was earlier. The test matrix employed in the present program is shown in Table 1, where σ_p is the proof stress and S is the (maximum) fatigue stress. Fatigue tests at $S/\overline{X} = 0.60$, 0.87 and 0.925 were carried out after proof tests to the respective fatigue stresses only.

Final failure modes were examined visually, and on a Scanning Electron Microscope (SEM) on a selective basis. A few specimens had one of the edges polished to monitor ply failures. Fatigue tests of these specimens were carried out intermittently to allow examinations of the edges on a microscope.

TABLE 1

TEST MATRIX

Test Series	Panel No.			
	10	11[a]	12	A
Strength				
Proof Stress $\sigma_p/\overline{X}$ [b]	0	0	0	0
	0.87	-	-	-
	0.95	-	-	-
Fatigue				
Fatigue Stress $S/\overline{X}$	0.80	0.70	0.87	0.60
	-	-	-	0.925
Proof Stress $\sigma_p/\overline{X}$	0.80	0.70	0.87	0.60
	0.87	0.87	-	0.925
	0.95	0.95	-	-

[a] $[0_2/90/\pm/\mp 45/90_2/0]$

[b] $\overline{X}$ is the average strength of each panel.

8

SECTION III

RESULTS AND DISCUSSIONS

1. STRENGTH AND LIFE DISTRIBUTIONS

The raw strength data are listed in Appendix A. These data are fit by a two-parameter Weibull distribution of the form

$$R_s(X) = \exp\left[-\left(\frac{X}{X_o}\right)^{\alpha_s}\right] \tag{1}$$

The shape parameter α_s and the characteristic strength X_o can be determined by the method of maximum likelihood [19]. The requisite equations are

$$\frac{1}{\alpha_s} = \frac{\displaystyle\sum_{i=1}^{m} X_i^{\alpha_s} \ln X_i}{\displaystyle\sum_{i=1}^{m} X_i^{\alpha_s}} - \frac{1}{m} \sum_{i=1}^{m} \ln X_i \tag{2}$$

$$X_o = \left[\frac{1}{m} \sum_{i=1}^{m} X_i^{\alpha_s}\right]^{1/\alpha_s} \tag{3}$$

In the above equations, X_i are the experimental data and m is the total number of samples.

Table 2 lists the values of α_s and X_o for the strength distributions of the panels used. There is little difference in α_s and X_o between

9

TABLE 2

MECHANICAL PROPERTIES OF PANELS

Panel No.	10	11	12	A
No. of Samples	20	20	8	20
Ultimate Stress				
α_s	19.08	1∧.81	30.94	21.45
X_o, MPa	811.97	629.48	796.49	806.93
Average $\overline{X}$, MPa	789.67	609.09	781.96	788.11
C. V., %	6.24	7.23	4.34	5.21
Ultimate Strain				
Average, mm/m	11.24	10.71	11.33	11.32
C. V., %	7.21	8.33	3.46	5.43
Modulus				
Average $\overline{E}$, GPa	68.36	57.23	69.44	69.74
C. V., %	6.03	4.54	2.64	4.86

panels 10 and A. Since panel 12 was used in Reference [18], only 8 specimens were tested from this panel. Although the present data gives the highest α_s for panel 12, the earlier data of Reference [18] yielded an α_s comparable to those of panels 10 and A. Furthermore, the characteristic strength X_o does not vary much amongst those three panels. The lack of panel-to-panel variability can also be seen from the ultimate strain and modulus data in Table 2.

Panel 11 has a lower shape parameter and a lower characteristic strength. A microscopic examination of this panel revealed that the actual layup was $[0_2/90/\pm45/\mp45/90_2/0]$ rather than the intended one of $[0_2/90/\pm45]_s$. Although this panel has only three 0-deg plies compared to four in the other panels, its characteristic strength is higher than three-fourths the average characteristic strength of the other three panels. Therefore, this panel 11 was also included in the test series.

The static strength distributions are shown in Figure 2. For the experimental data the median rank was used to represent the probability of survival, i.e.,

$$R_s(X_i) = 1 - \frac{i-0.3}{m+0.4} \tag{4}$$

Note that now X_i is the i-th strength, not an arbitrary strength as in Equations (2) and (3).

The fatigue life data at the five different stress levels are shown in Figure 3. The corresponding numerical data can be found in

11
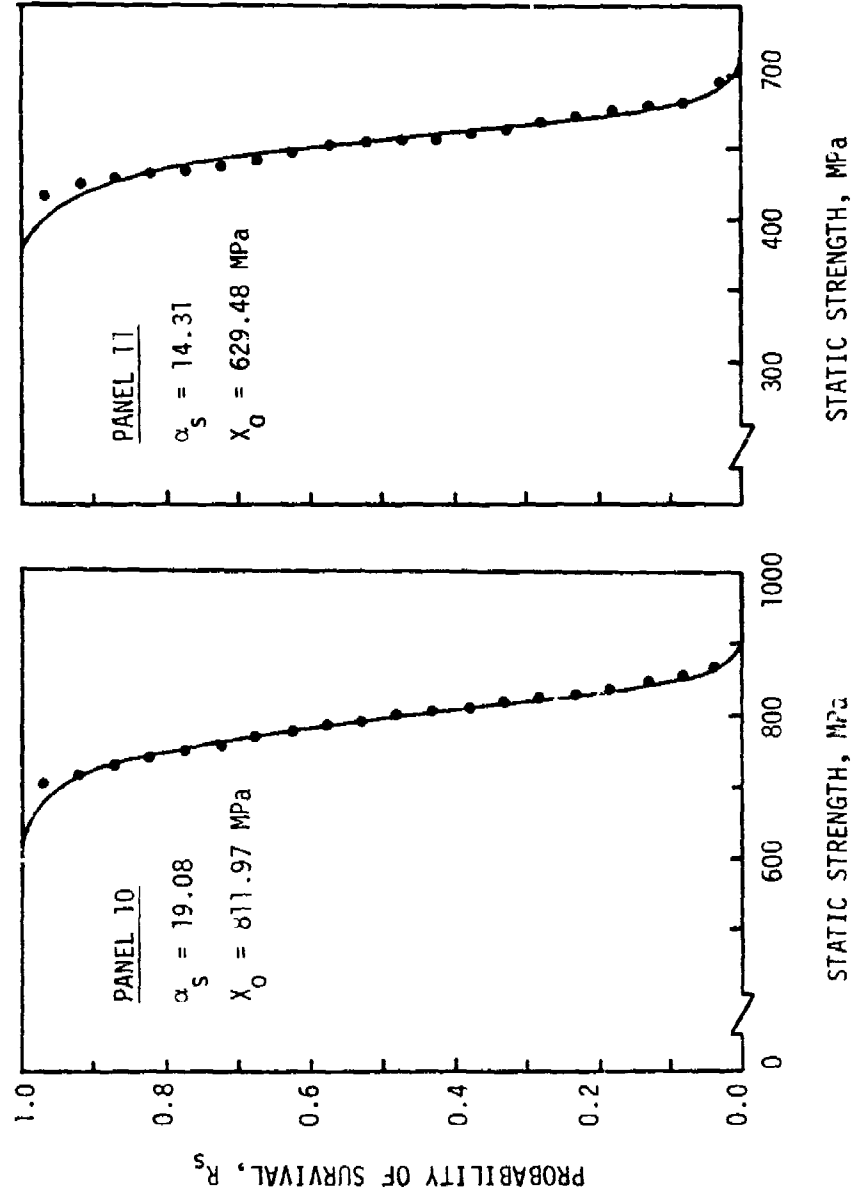
Figure 2a. Static Strength Distributions: Panels 10 and 11.

12
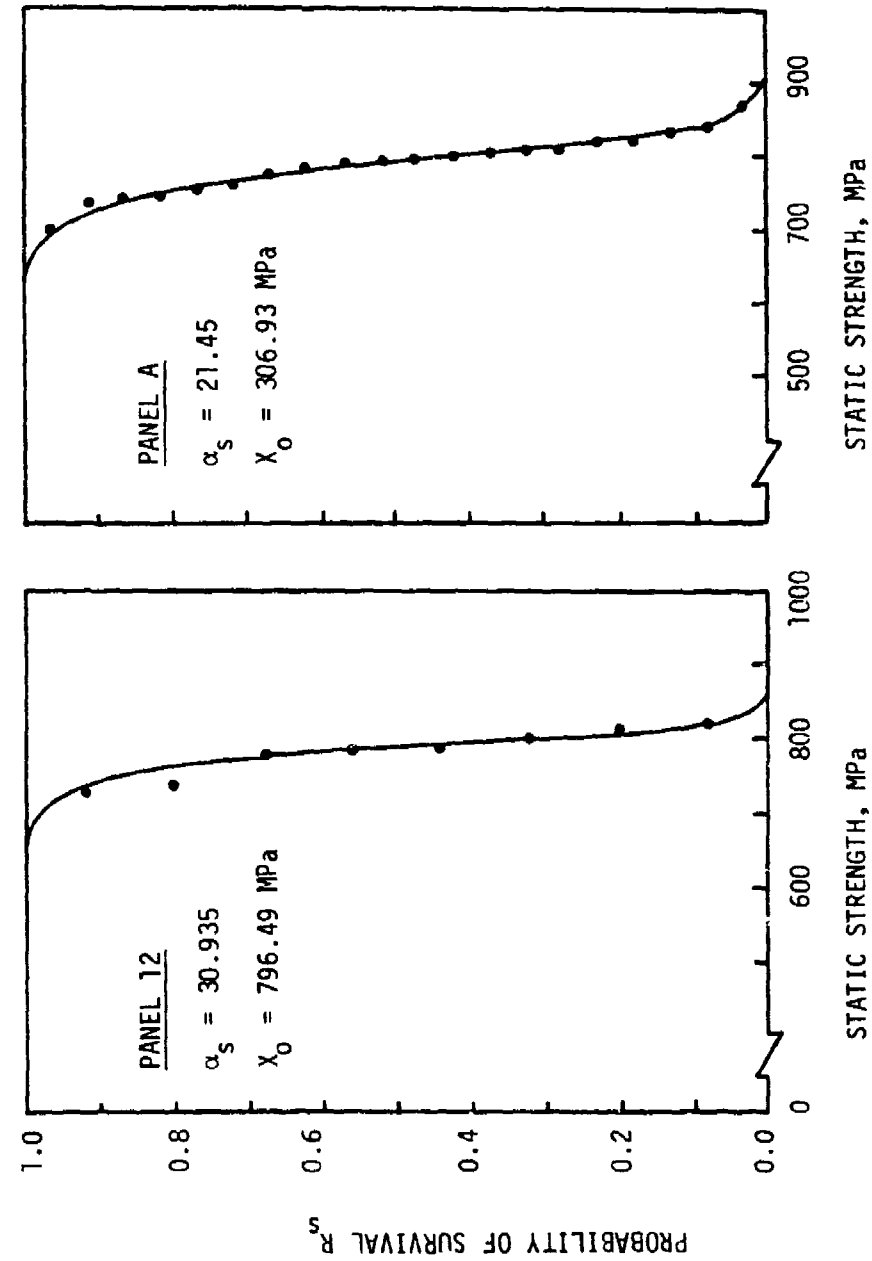
Figure 2b. Static Strength Distributions: Panels 12 and A.
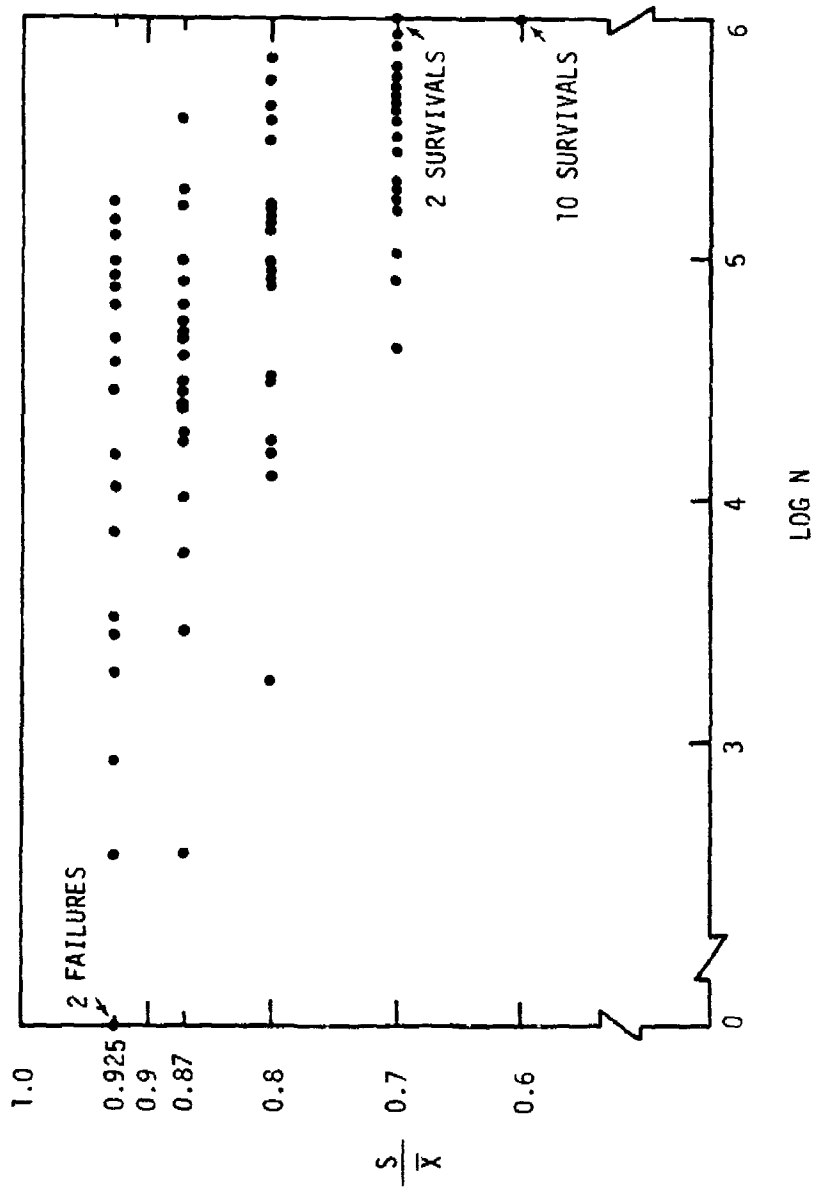
Figure 3. Fatigue Stress-Life (S-N) Relation.

14

Appendix B. Note that these fatigue tests were preceded by a proof test to each maximum fatigue stress.

The fatigue data are again fit by a two-parameter Weibull distribution:

$$R_f(N) = \exp\left[-\left(\frac{N}{N_o}\right)^{\alpha_f}\right] \tag{5}$$

The equations for the shape parameter α_f and the characteristic lifetime N_o are slightly different from Equations (2) and (3) because some specimens survived 10^6 cycles at which testing was stopped. In terms of the run-out cycles N_r and the number of failures r, they are

$$\frac{1}{\alpha_f} = \frac{\sum_{i=1}^{r} N_i^{\alpha_f} \ln N_i + (m-r) N_r^{\alpha_f} \ln N_r}{\sum_{i=1}^{r} N_i^{\alpha_f} + (m-r) N_r^{\alpha_f}} - \frac{1}{r} \sum_{i=1}^{r} \ln N_i \tag{6}$$

$$N_o = \left[\frac{1}{r} \sum_{i=1}^{r} N_i^{\alpha_f} + (m-r) N_r^{\alpha_f}\right]^{1/\alpha_f} \tag{7}$$

The parameters α_f and N_o at the fatigue stresses of 0.70 $\overline{X}$, 0.80 $\overline{X}$ and 0.87 $\overline{X}$, are listed in Table 3. At 0.925 $\overline{X}$ these parameters were not determined because two specimens failed during proof tests as would be expected from the static strength distribution. In such case, Equation (5) must be modified. One candidate distribution is [11]

15

TABLE 3

FATIGUE LIFE PARAMETERS

Fatigue Stress, $S/\bar{X}$	Total No. of Specimens	No. of Failures	α_f	N_o
0.60	10	0	-	-
0.70	20	18	1.504	473,483
0.80	20	20	0.882	167,052
0.87	20	20	0.819	60,030
0.925	20	20	-	-

$$R_f(N) = \exp\left\{-\left[\left(\frac{S}{X_o}\right)^{\alpha_s/\alpha_f} + \frac{N}{N_o}\right]^{\alpha_f}\right\} \qquad (8)$$

The foregoing equation correctly satisfies the limiting condition that

$$R_f(0) = R_s(S) \qquad (9)$$

The present parameters in Table 3 are compared in Figures 4 and 5 with those for quasi-isotropic laminates of References [7,20]. These laminates are $[0/90/\pm45]_s$ T300/5208 in Reference [7] and $[45/(90/-45)_2/0/45/0]_s$ T300/934 in Reference [20]. The results of Reference [20] are based on the data from Reference [21]. Note that, in all cases, α_f is larger at lower stresses. In fact, the same trend was observed in the stress-rupture data for glass/epoxy and Kevlar 49/epoxy strands [22]. For the present laminate the characteristic life is seen to increase more slowly as the fatigue stress is lowered. However, it should be noted that all ten specimens tested at 0.60 $\overline{X}$ survived 10^6 cycles.

The fatigue life distributions are shown in Figure 6. Again, the two-parameter Weibull distribution, Equation (5), can describe the life data very well.

2. EFFECT OF PROOF TEST ON STRENGTH

From panel 10, twenty specimens were proof-tested to 0.87 $\overline{X}$, and twenty-five specimens to 0.95 $\overline{X}$. None of the specimens failed during the proof test to 0.87 $\overline{X}$. However, seven specimens failed before reaching 0.95 $\overline{X}$. The respective numbers of failures can be calculated from the strength distribution (1) and the median rank (4) as follows:

17
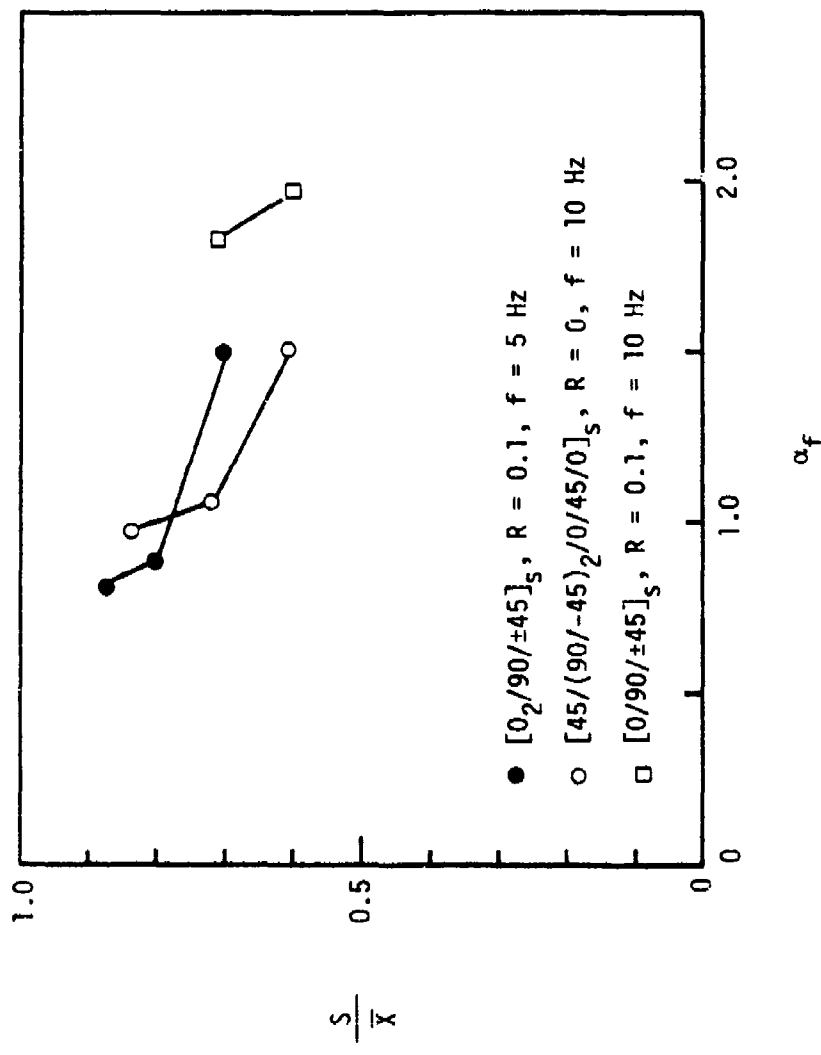
Figure 4. Effect of Fatigue Stress on Shape Parameter.
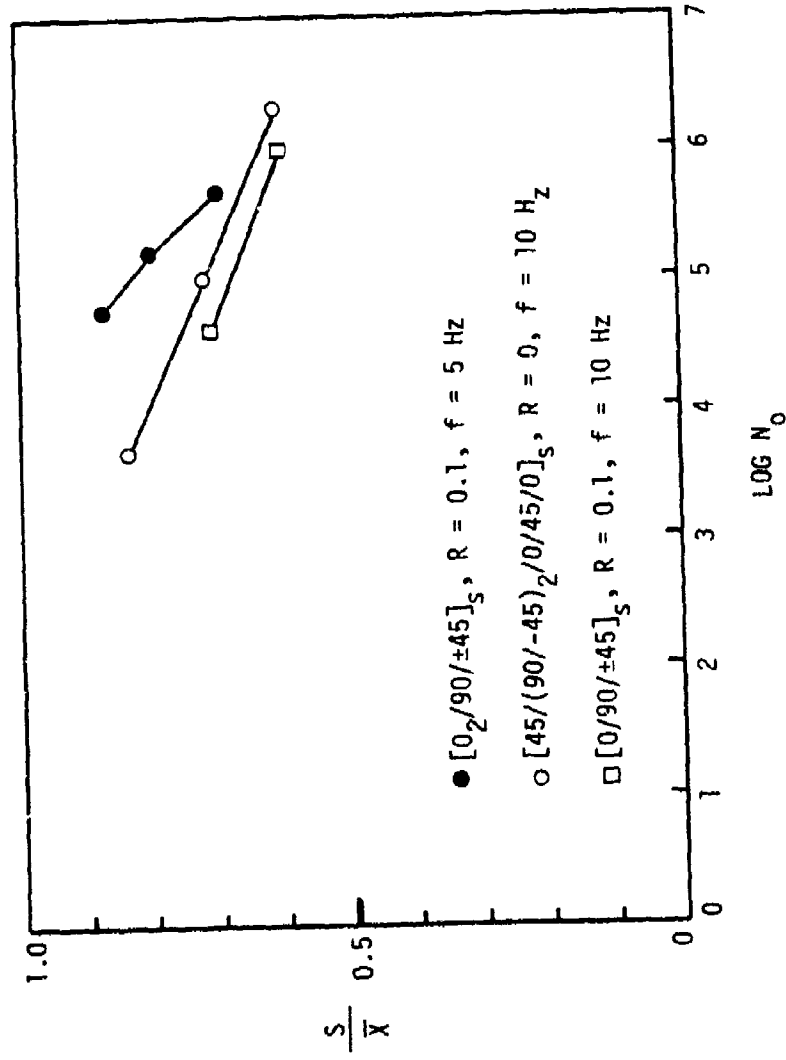
Figure 5. Effect of Fatigue Stress on Characteristic Life.

● $[0_2/90/\pm45]_s$, R = 0.1, f = 5 Hz

○ $[45/(90/-45)_2/0/45/0]_s$, R = 0, f = 10 Hz

□ $[0/90/\pm45]_s$, R = 0.1, f = 10 Hz

LOG N_0

$\frac{S}{X}$
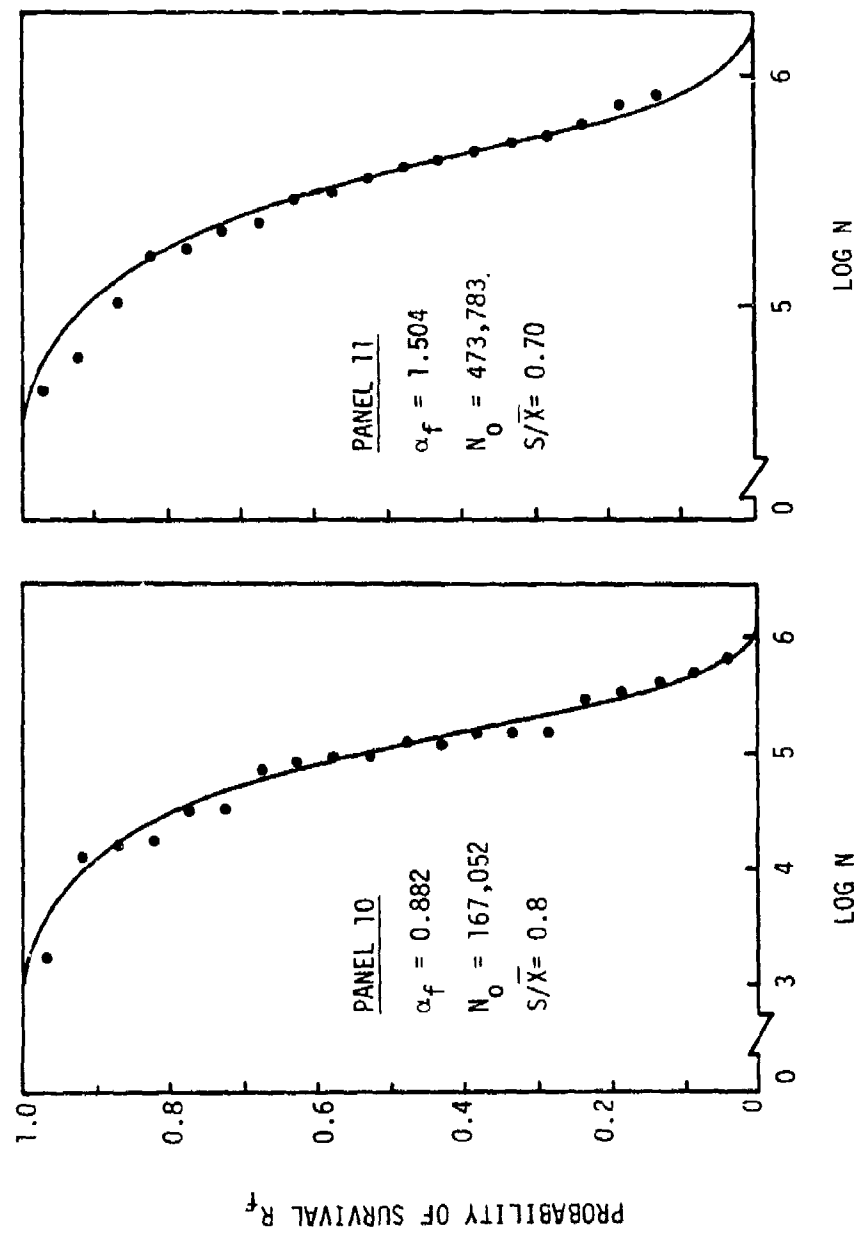
Figure 6a. Life Distributions: $S/\overline{X}$ = 0.70 and 0.80.

The figure contains two panels with the following labels:

PANEL 10
α_f = 0.882
N_o = 167,052
$S/\overline{X}$ = 0.8

PANEL 11
α_f = 1.504
N_o = 473,783.
$S/\overline{X}$ = 0.70

Axis labels: PROBABILITY OF SURVIVAL R_f (vertical), LOG N (horizontal)
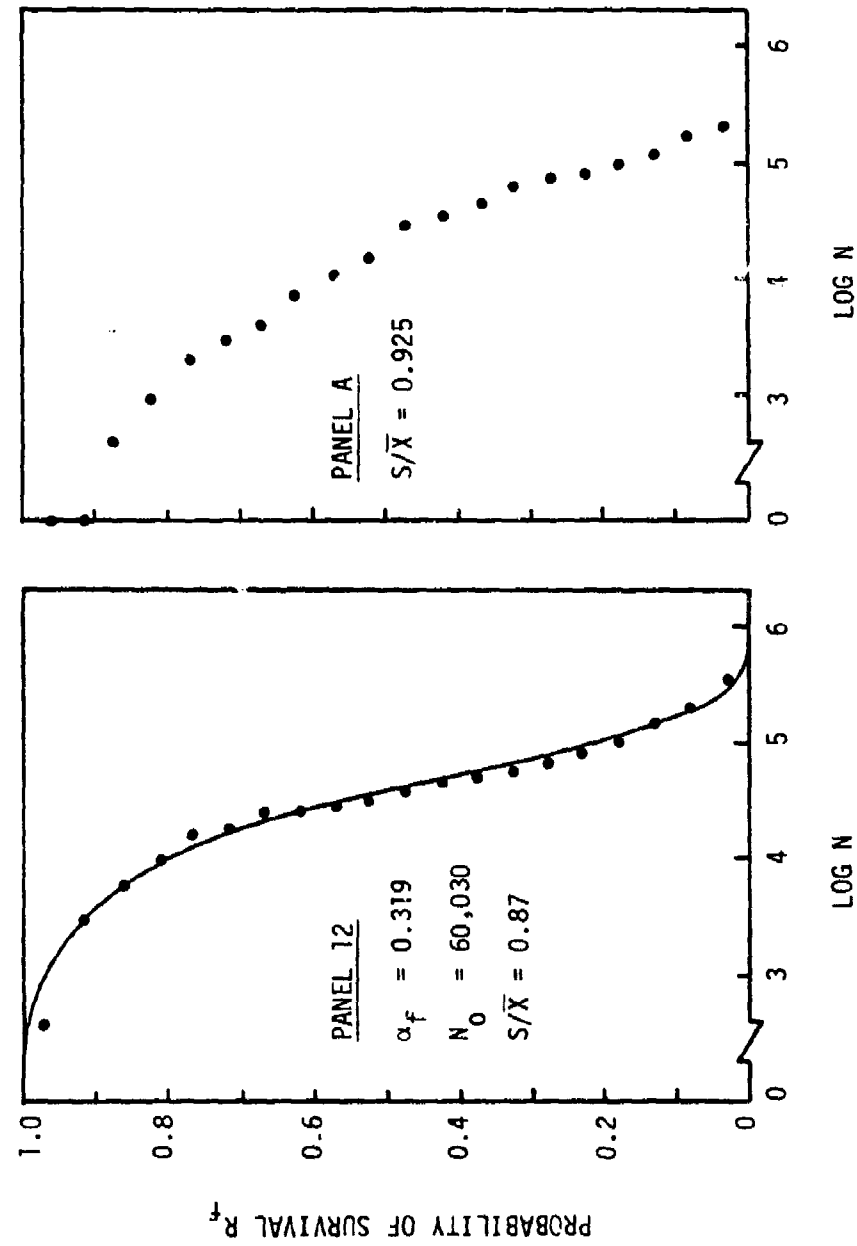
Figure 6b.   Life Distributions: $S/\overline{X}$ = 0.87 and 0.925.

21

Number of failures to 0.87 $\overline{X}$ = 1.1

Number of failures to 0.95 $\overline{X}$ = 5.3

Thus, the prediction is higher for 0.87 $\overline{X}$ and lower for 0.95 $\overline{X}$.

The post-proof strength data, listed in Appendix C, are compared with the initial strength distribution in Figure 7. After proof test to 0.87 $\overline{X}$ the residual strengths are slightly higher than the initial strengths, in the lower strength region. However, an opposite trend is observed in the higher strength region. When the proof stress is 0.95 $\overline{X}$, the residual strengths are consistently lower than the initial strengths, although the difference is rather small.

It should be noted that in both cases the lowest residual strengths are higher than the respective proof stresses. This observation is in contrast to the results reported in Reference [7] where some of the residual strengths were lower than the proof stresses.

In light of the foregoing observations we can conclude that the proof tests employed in the present program have little effect on the residual strength.

3.   EFFECT OF PROOF TEST ON LIFE

In this test series specimens were first proof-tested to a predetermined stress level and then fatigued to failure or 10^6 cycles whichever occurred earlier. The appropriate stress levels and the corresponding numbers of specimens are listed in Table 4.

The actual number of failures during each proof test is comparable to those predicted from Equations (1) and (4), as shown in Table 4.

22
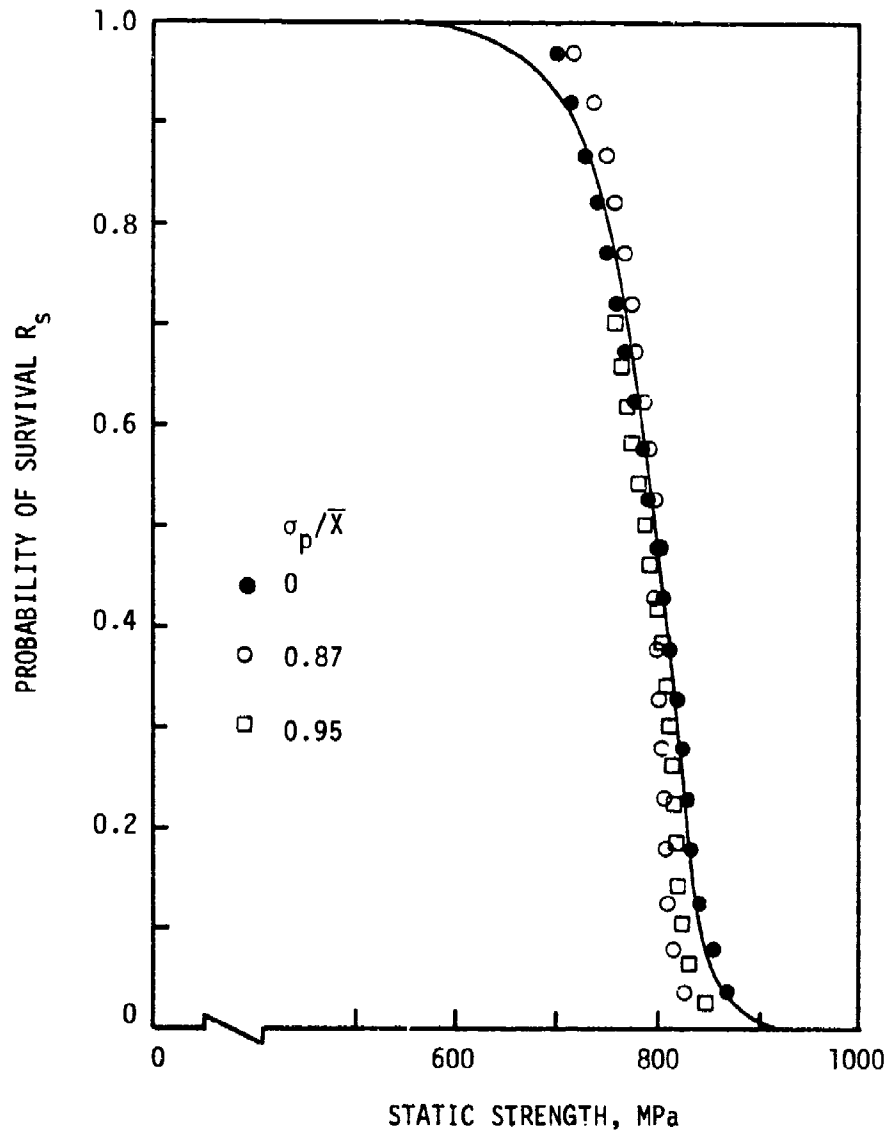
Figure 7.   Effect of Proof Test on Strength.

TABLE 4

FAILURE DURING PROOF TEST

Fatigue Stress/$\overline{X}$	Proof Stress/$\overline{X}$	Number of Specimens	Number of Failures During Proof Test	Calculated No. of Failures During Proof Test
0.7	0.87	20	1	1.8
	0.95	20	5	5.4
0.8	0.87	21	1	1.2
	0.95	20	5	4.3

24

Since the same panel 10 was used for both Section 3.2 and the fatigue stress of 0.8 $\overline{X}$ in Table 4, we can combine the two sets of data to get the total numbers of failures. At $\sigma_p/\overline{X} = 0.87$, the actual number of failures is 1 out of 41 while the predicted is 2.0. At $\sigma_p/\overline{X} = 0.9^-$, there are more failures than predicted; 12 compared to 9.3 out of 45.

The residual lives after proof test, listed in Appendix D, are compared with the initial lives in Figures 8 and 9. At $S/\overline{X} = 0.70$, proof tests to higher than the fatigue stress result in longer residual lives. At the higher fatigue stress of $0.80\ \overline{X}$, however, the residual lives are reduced by the proof tests especially in the shorter life region.

The two sets of data in Figures 8 and 9 are also contradictory to each other as regards the effect of the proof stress level. In Figure 8, the higher proof stress seems more deleterious; however, quite the opposite is observed in Figure 9. Therefore, it is possible that the differences between the initial life data and the residual life data are the result of sampling variation.

4. STRENGTH-LIFE RELATIONS

Recent investigations [2-7] suggested the existence of a relationship between strength and life for composite laminates. The possibility of such a relationship is investigated in the present section.

Consider the set of ordered strengths $\{X_i; i=1, 2, \ldots, m\}$ and the set of ordered lives $\{N_i; i=1, 2, \ldots, m\}$ at a fatigue stress. The fatigue stress is low enough so that no failure occurs in proof test to this level. If strength is related to life such that a statically

25
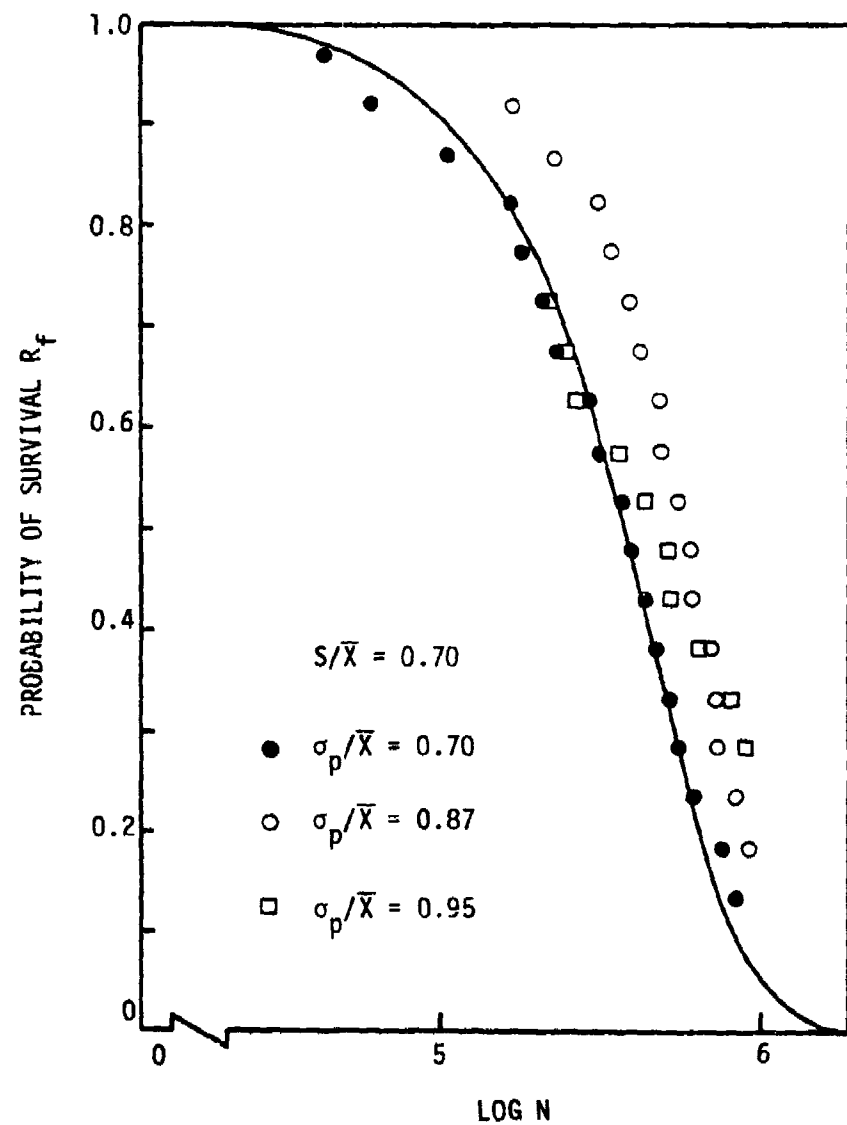
Figure 8. Effect of Proof Test on Life, $S/\overline{X} = 0.70$.

The figure shows a plot of PROBABILITY OF SURVIVAL R_f (vertical axis, from 0 to 1.0) versus LOG N (horizontal axis, from 0 to 6).

Legend:
$S/\overline{X} = 0.70$

● $\sigma_p/\overline{X} = 0.70$
○ $\sigma_p/\overline{X} = 0.87$
□ $\sigma_p/\overline{X} = 0.95$
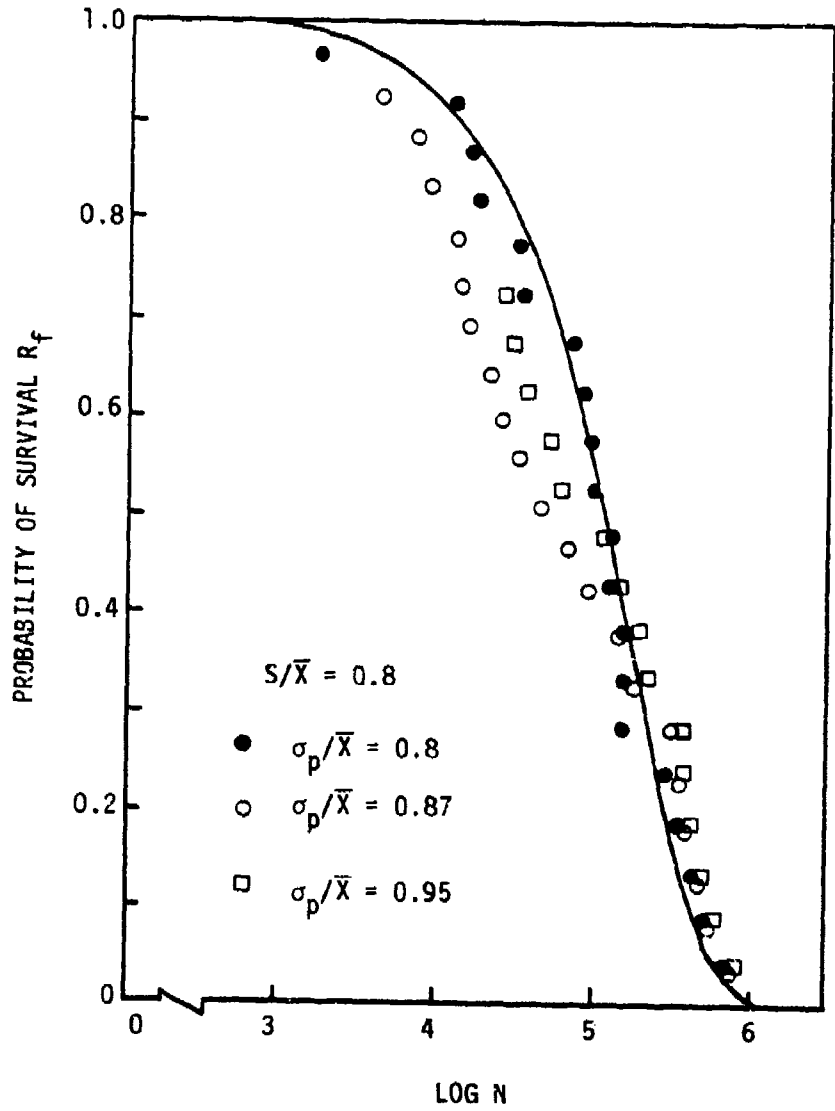
Figure 9. Effect of Proof Test on Life, $S/\overline{X} = 0.80$.

stronger specimen has a longer life, the strength-life relationship

is represented by the set of pairs $\{(X_i, N_i); i=1, 2, \ldots, m\}$. Such

relationship is shown in Figure 10 for $S/\overline{X} = 0.70$ and in Figure 11 for

$S/\overline{X} = 0.80$. Also shown in the figures at the ordinates equal to the

proof stress levels are the residual life data.

Suppose a specimen survives a proof test to a stress σ_p. Its

strength is then higher than σ_p. If the strength-life relation is

as shown in, say, Figure 10 at $S/\overline{X} = 0.70$, the life of the specimen

should not be shorter than the life corresponding to σ_p on the

ordinate as long as the proof test does not cause any critical damage.

Since the effect of proof test has already been found to be

negligible in Section 3.3, the residual life data plotted at $\sigma_p/\overline{X} = 0.87$

and 0.95 can be taken as a proof for the hypothesized strength-life

relation to be a real one. The same conclusion can be drawn from

Figure 11 for the fatigue stress of $0.80 \overline{X}$.

Analytically, the strength-life relations can be obtained from

Equations (1) and (5) by noting that a strength in the strength

population is paired with the life of the same rank in the life

population. That is,

$$R_s(X) = R_f(N) \tag{10}$$

Therefore,

$$\frac{X}{X_o} = (\frac{N}{N_o})^{\alpha_f/\alpha_s} \tag{11}$$

28
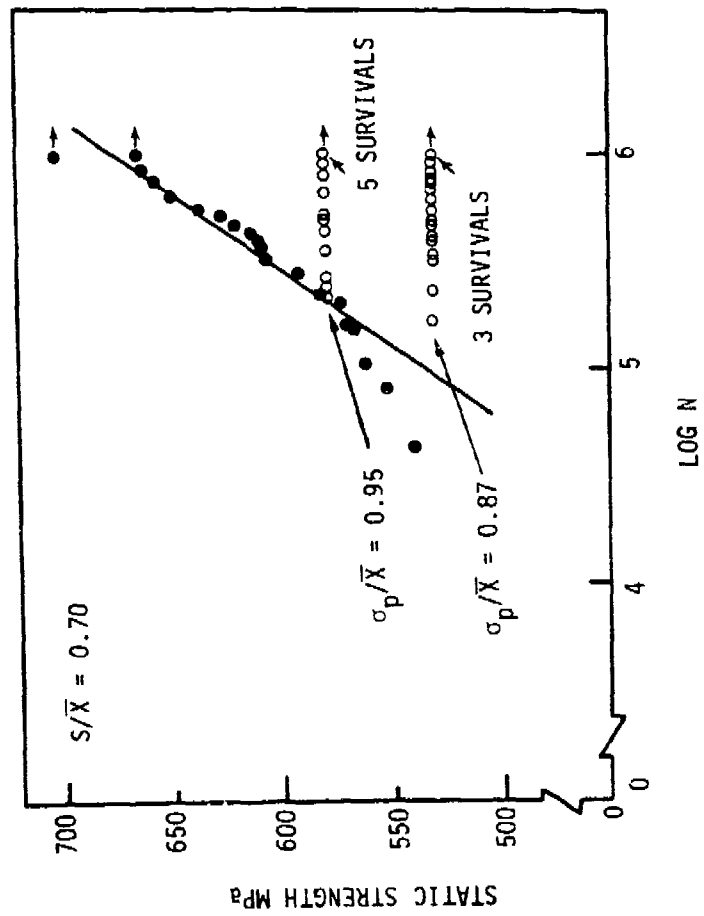
Figure 10. Strength-Life Relation at $S/\overline{X} = 0.70$.
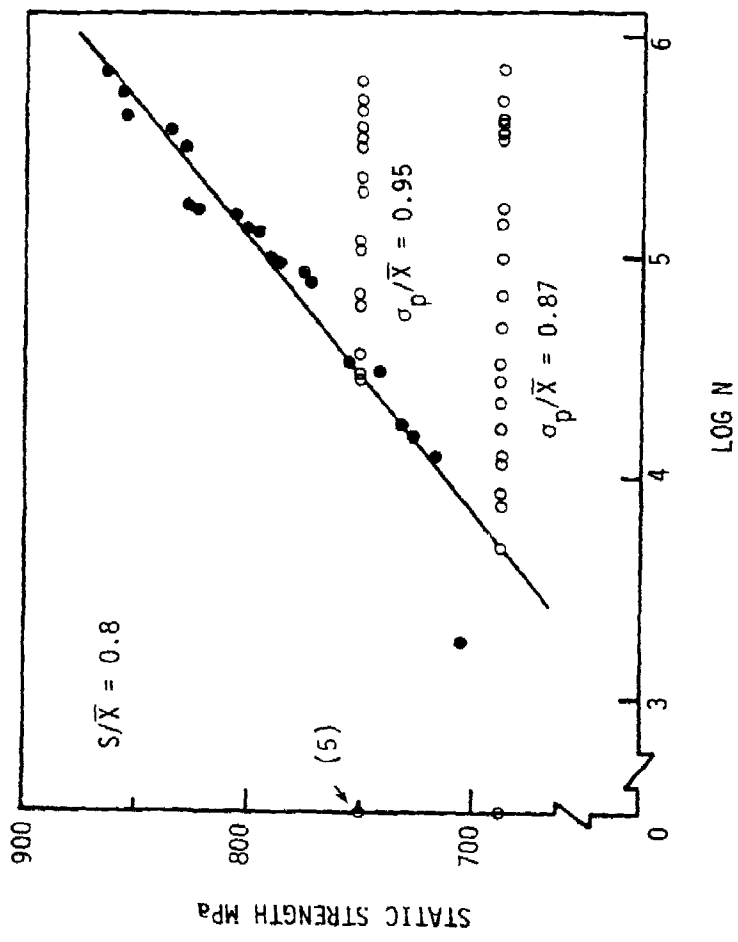
Figure 11. Strength-Life Relation at $S/\bar{X} = 0.80$.

As remarked earlier, Equation (5) is valid if the fatigue stress is so low that the static failures up to this stress are negligiole. Otherwise, Equation (8) must be used in lieu of Equation (10). The new equation is thus

$$\frac{X}{X_o} = \left[(\frac{S}{X_o})^{\alpha_s/\alpha_f} + \frac{N}{N_o} \right]^{\alpha_f/\alpha_s} \tag{12}$$

Note that Equation (12) correctly suggests that only those strengths higher than the fatigue stress can be related to the life data.

In the present case, Equation (11) can be used; it is shown in Figures 10 and 11 for $S/\overline{X} = 0.70$ and 0.80, respectively. The actual minimum residual lives are very close to the predicted values except at $S/\overline{X} = 0.70$ and $\sigma_p/\overline{X} = 0.87$ where the prediction is quite conservative.

References [3,4,6,7] report a number of premature failures before reaching the minimum lifetimes guaranteed by proof tests. Figures 10 and 11, however, show no noticeable premature failures.

5.   MODULUS-STRENGTH AND -LIFE CORRELATIONS

Figure 12 shows stress-strain relations for a specimen from panel 11. The strains were measured with strain gages. Note that the axial strain is quite linear up to failure while the lateral (Poisson) strain shows a slight nonlinearity.

During each proof test the axial strain was measured with an extensometer. As with a strain gage in Figure 12, the axial strains were quite linear. Therefore, the corresponding axial modulus was simply calculated as the ratio of the proof stress to the corresponding
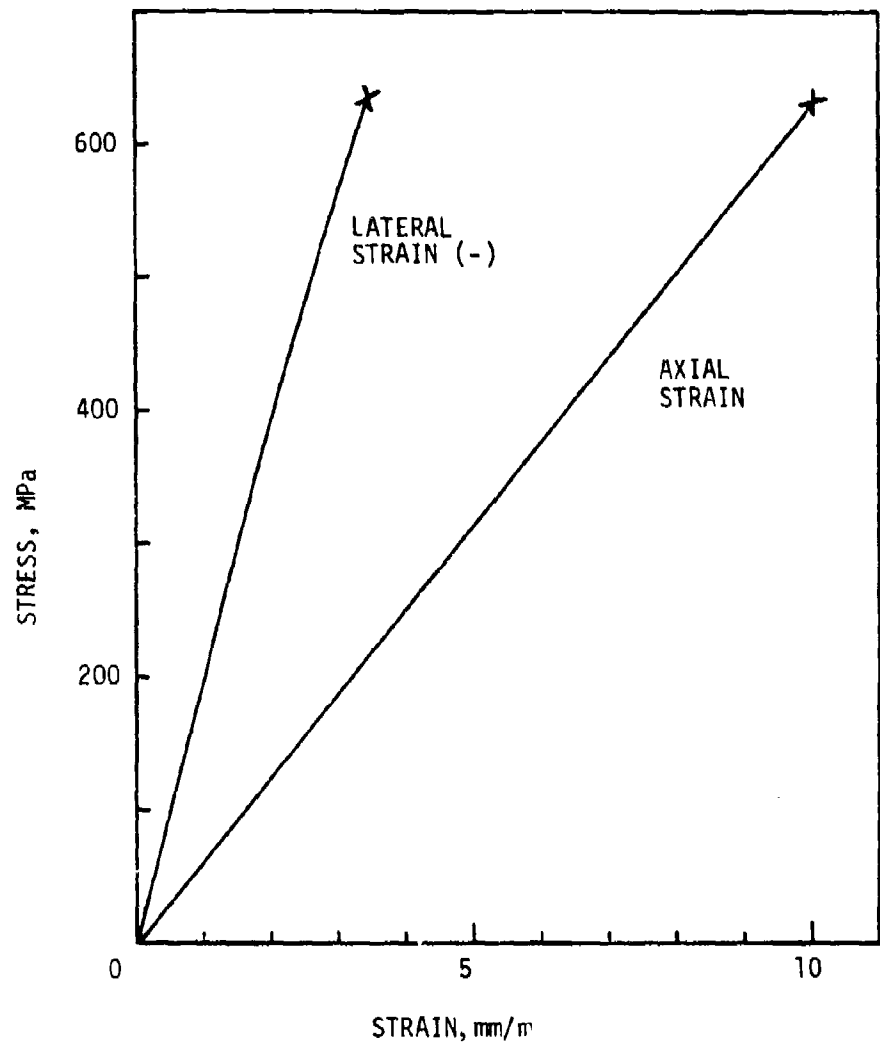
Figure 12. Stress-Strain Relations in a Static Tension.

strain measured. The modulus data are included in Appendices A
through D.

Figure 13 shows the moduli versus the static strengths for
panels 10, 11, 12 and A. A better correlation between the modulus and
strength is seen for panels 11 and A. Yet, there is a definite trend
that a higher modulus is an indication of a higher strength in all the
panels.

Surprisingly, a better correlation is seen between the modulus
and life, Figure 14, regardless of the fatigue and proof stress levels.
The combined results of Figures 13 and 14 give additional credence to
the strength-life relations discussed in Section 3.4.

It is plausible to assume that a higher modulus is a manifestation
of a higher fiber volume content. Therefore, one can justifiably
expect that a specimen with higher modulus will have a higher strength
and longer fatigue life.

6. LIFE-FAILURE MODE CORRELATION

A typical static failure mode in Figure 15 is characterized by a
relative lack of delamination except very near the fracture site. In
fatigue, however, extensive delamination is usually observed between
plies with different orientations, Figure 16. Most frequent delamination
is either between the 0-deg and 90-deg plies or between the 90-deg and
45-deg plies. However, the +45-deg plies can also be separated from
the -45-deg plies as shown in Figure 17.

To investigate when the final failure mode changes from a static
one to one of a typical fatigue failure, each failed specimen was

33
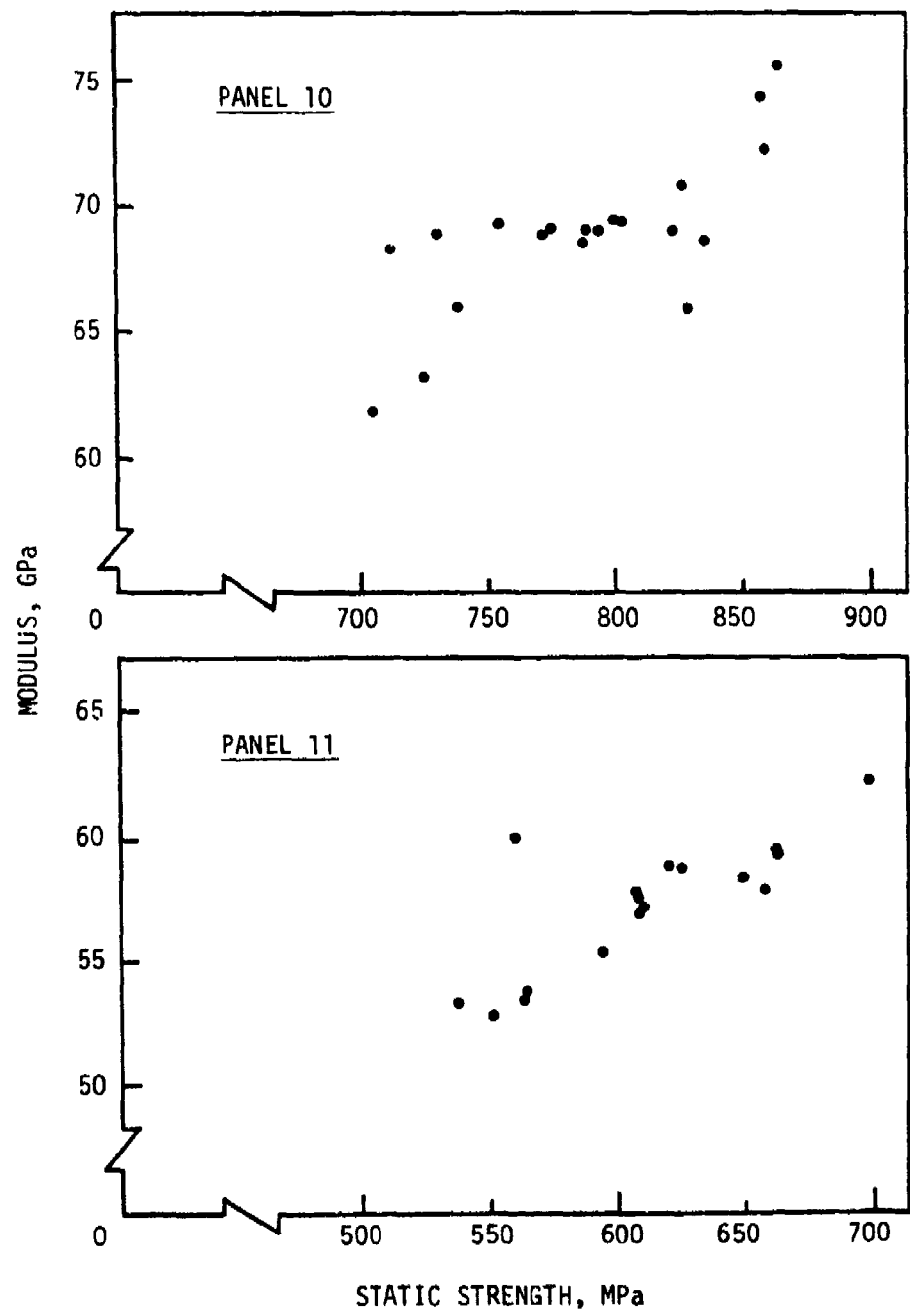
Figure 13a. Modulus-Strength Correlations: Panels 10 and 11.

34
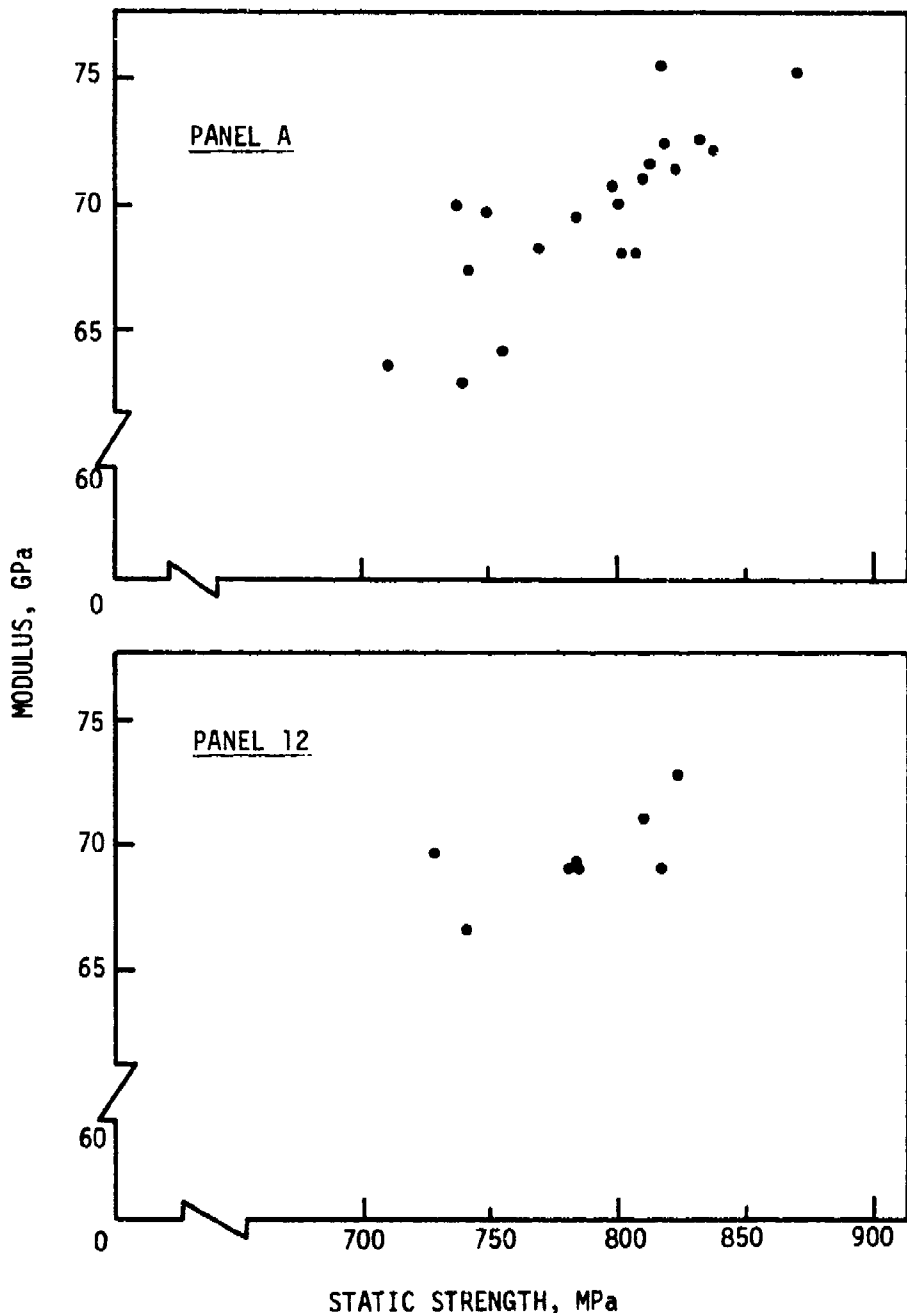
Figure 13b. Modulus-Strength Correlations. Panels 12 and A.

35
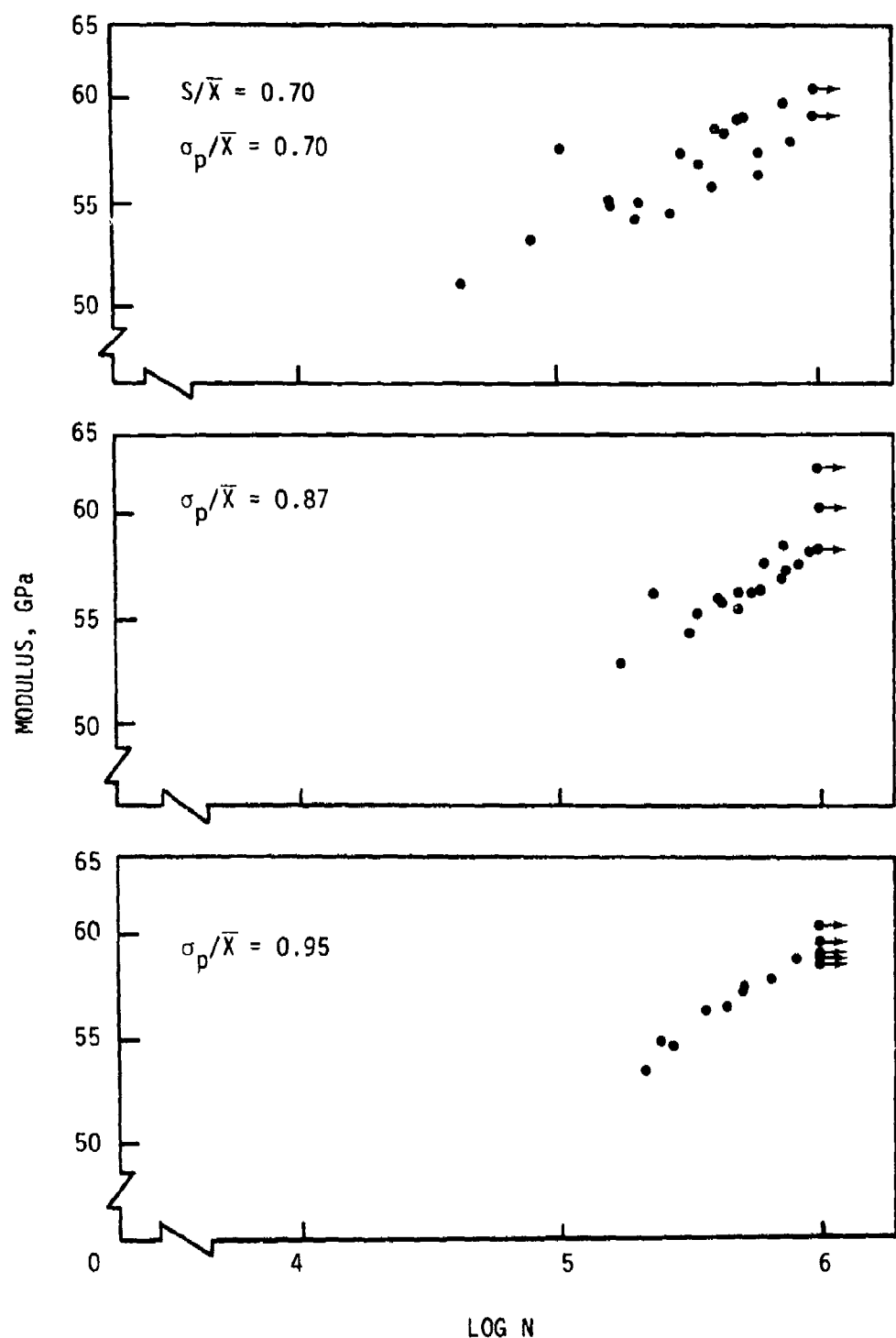
Figure 14a.   Modulus-Life Correlations: $S/\overline{X} = 0.70$.
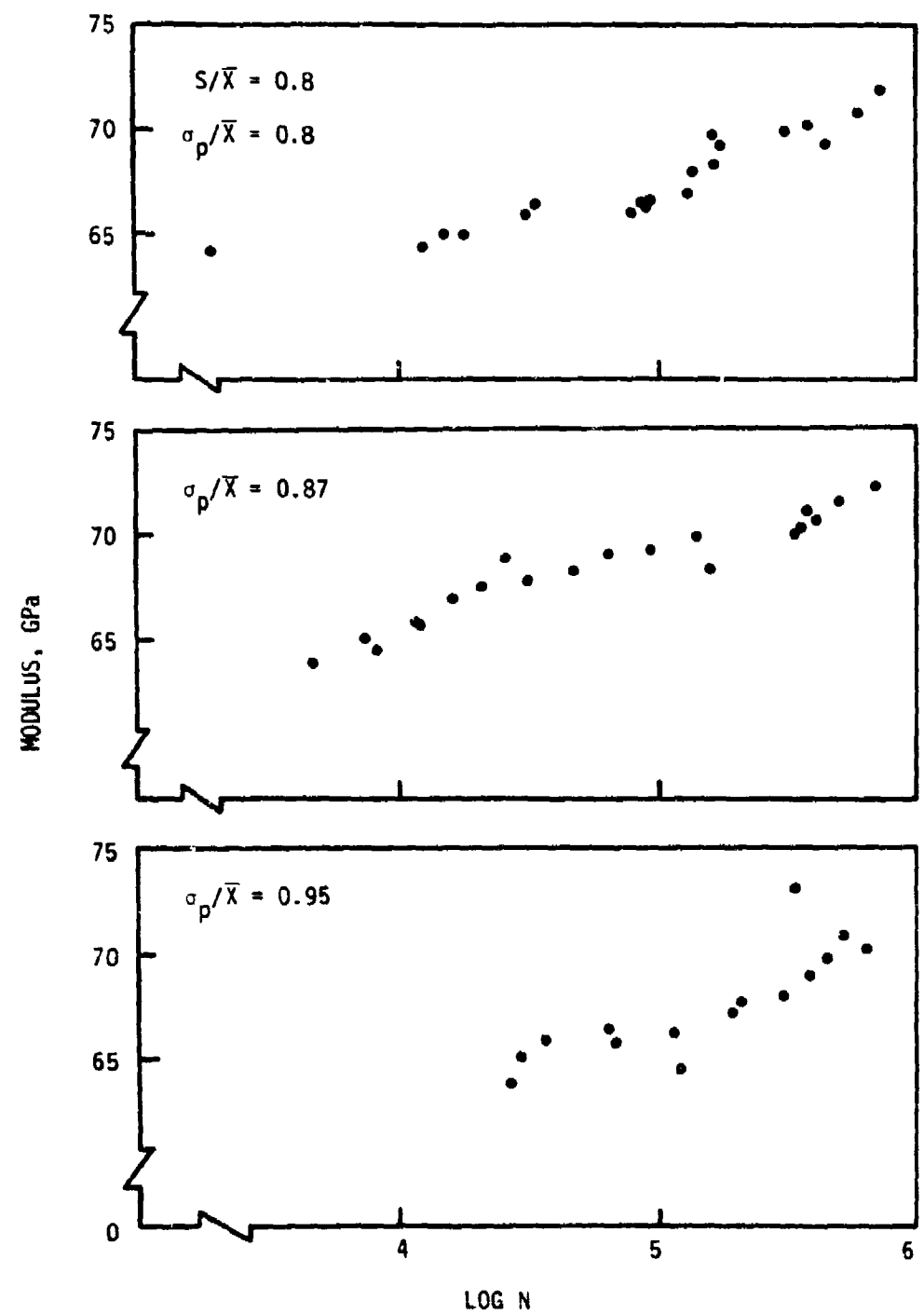
Figure 14b. Modulus-Life Correlations: $S/\overline{X} = 0.80$.
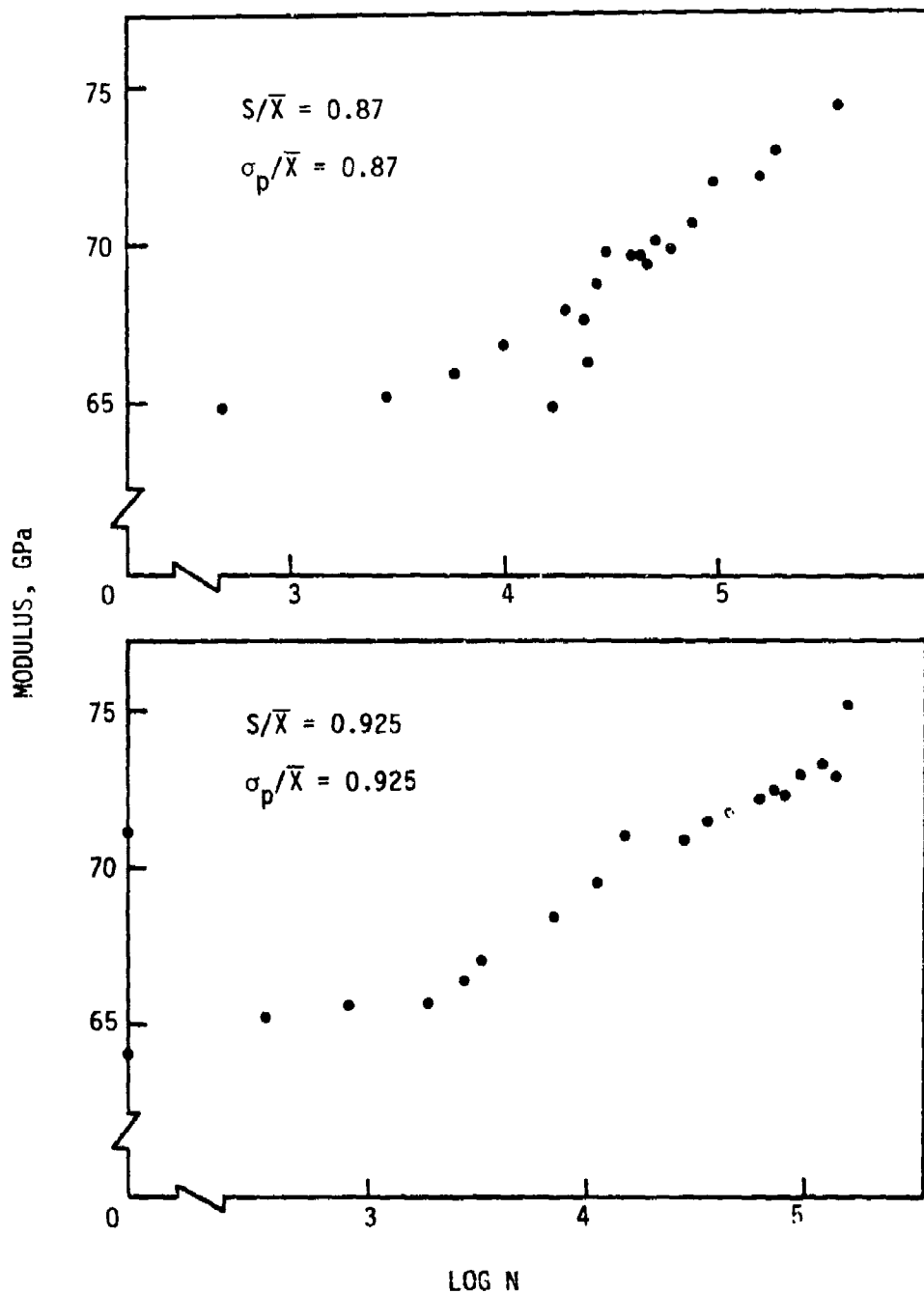
Figure 14c. Modulus-Life Correlations: $S/\overline{X} = 0.87$ and 0.925.
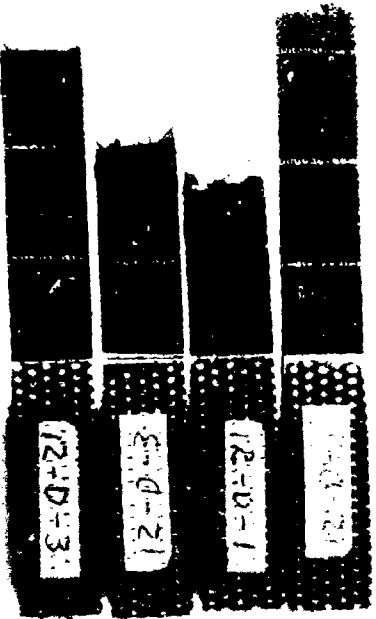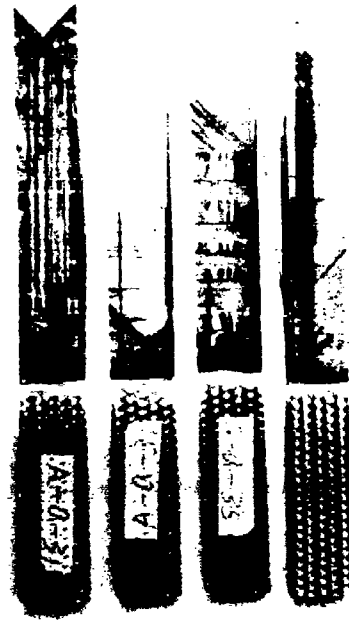
Figure 15. Typical Static Failure Modes.

A-a-31   A-a-35

Figure 16.   Typical Fatigue Failure Modes: $S/\overline{X} = 0.925$;
              $N = 64,847$ cycles for A-a-31; $N = 57,112$ cycles
              for A-a-35.

Figure 17. Extensive Delamination: $S/\overline{X} = 0.80$, $\sigma_p/\overline{X} = 0.95$, $N = 315,835$ cycles.

examined as to the severity of delamination. The results are shown in Figures 18 through 20.

At $S/\overline{X} = 0.70$, Figure 18, all specimens except only a few showed extensive delamination. One specimen which retained about 30% of the static failure mode is shown in Figure 21. However, most specimens, when failed, looked like those in Figure 22. The typical delamination before final failure is shown in Figure 23. In some specimens, delamination was coupled with longitudinal cracks in the 0-deg plies as shown in Figure 24. Note that, if delamination occurs between a 90-deg ply and the neighboring 45-deg ply, the 0-deg plies will be subjected to a transverse tension-tension fatigue because of the mismatch in Poisson's ratio between the 0-deg and 90-deg plies.

The most interesting change in the final failure mode occurs at the fatigue stress of $0.80 \overline{X}$, Figure 19. Here, if a specimen fails before about 20,000 cycles, its final failure mode is more like a static failure. However, if a specimen survives this threshold number of cycles, it undergoes extensive delamination before the final failure. In Figure 25, the specimen on the left-hand side shows a 100% fatigue failure mode while the other one shows only 40% of the fatigue failure mode.

At $S/\overline{X} = 0.87$, the final failure mode changes over a wide region, Figure 20. Furthermore, no fatigue failure looked exactly like a static failure. Figure 26 shows two types of failure modes: 100% fatigue failure on the left and 60% fatigue failure on the right.

42
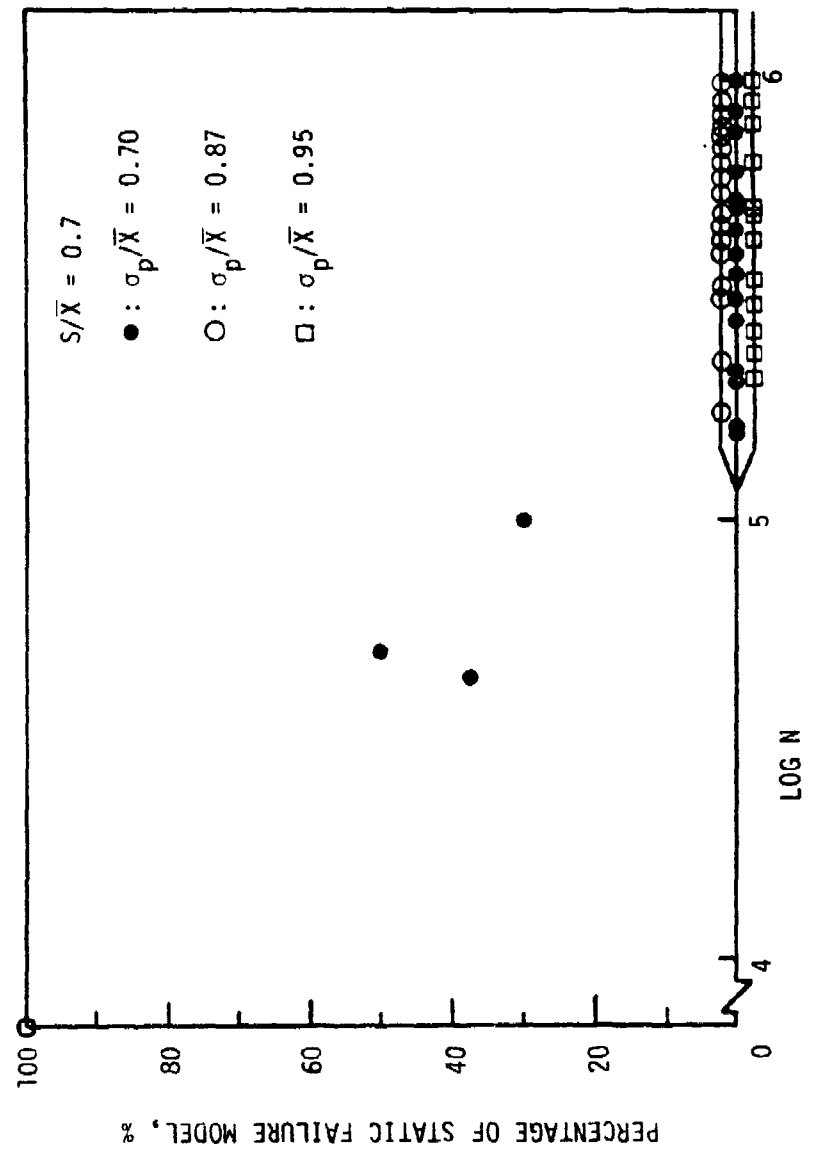
Figure 18. Failure Mode-Life Correlation: $S/\overline{X} = 0.70$, $\sigma_p/\overline{X} = 0.70$, 0.87 and 0.95.

43
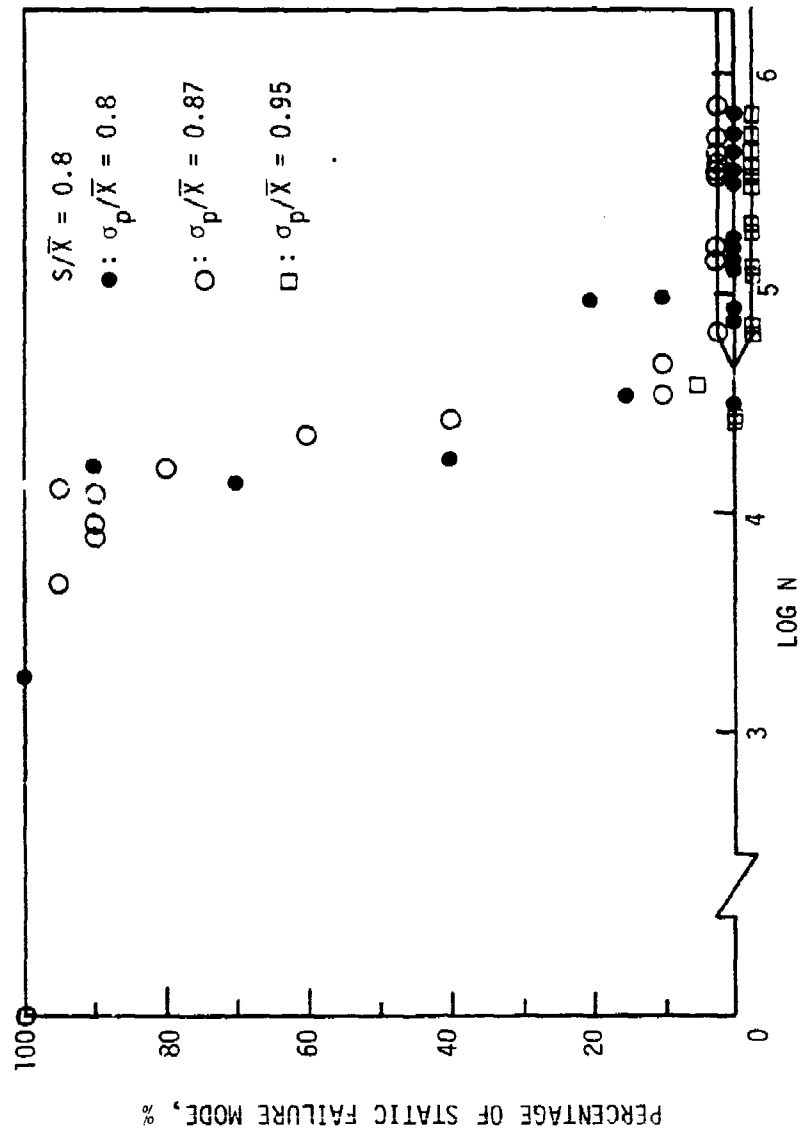
Figure 19. Failure Mode-Life Correlation: $S/\overline{X} = 0.80$, $\sigma_p/\overline{X} = 0.80$, 0.87 and 0.95.

44
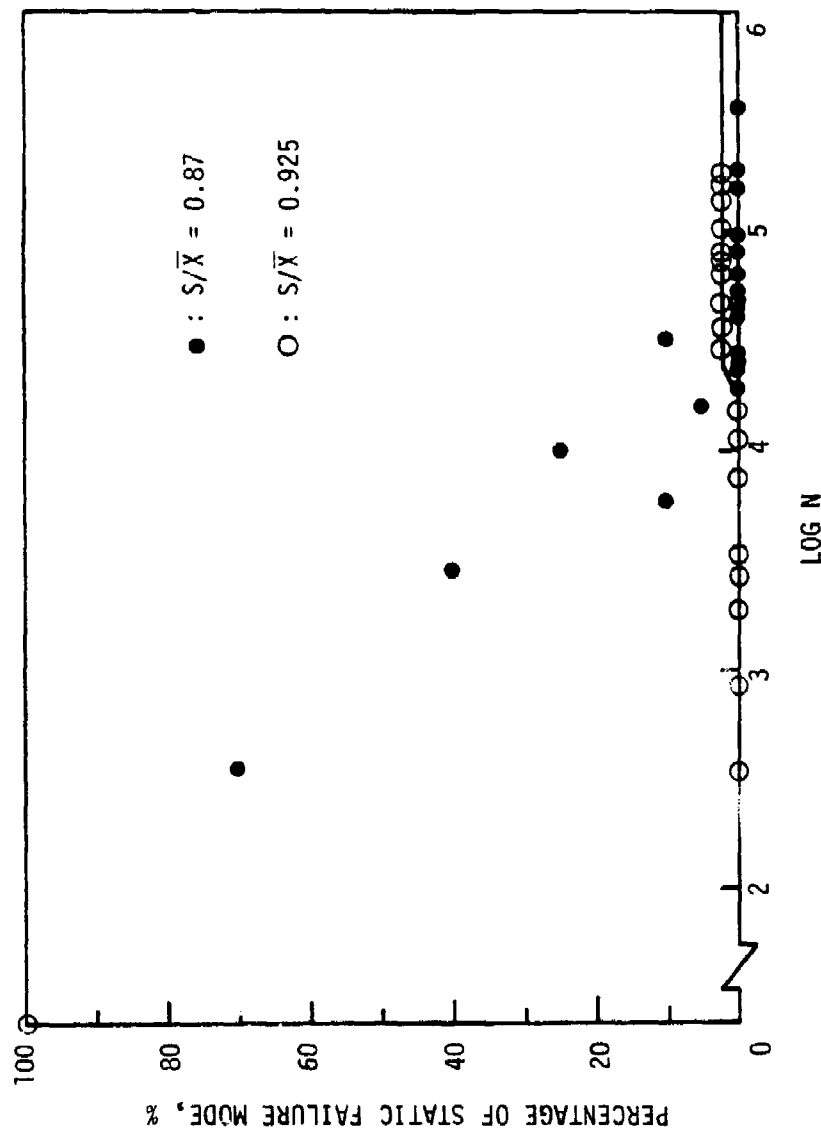
Figure 20. Failure Mode-Life Correlation: $S/\overline{X} = 0.87$ and 0.925.

45
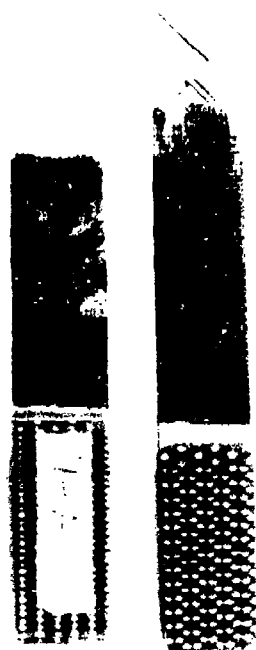
Figure 21. Fatigue Failure Showing 30% Static Failure Mode:
$S/\bar{X} = 0.70$, $N = 107,387$ cycles.

11-C-15   11-C-17   11-C-18

Figure 22.   Failure Modes at $S/\overline{X} = 0.70$, $\sigma_p/\overline{X} = 0.87$:
N = 735,134 cycles for 11-C-15; N = 409,216
cycles for 11-C-17; N = 498,211 cycles for
11-C-18.

11-D-13   11-C-20
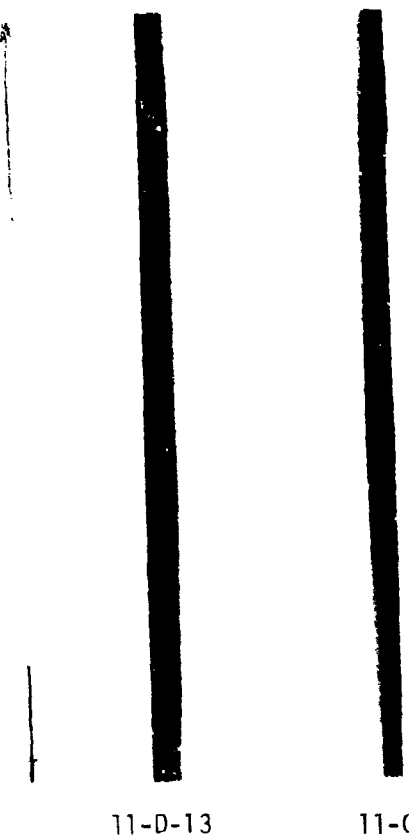
Figure 23.   Delaminations in Run-Out Specimens at $S/\overline{X} = 0.70$:
             $\sigma_p/\overline{X} = 0.95$ for 11-D-13 and 11-C-20.

48
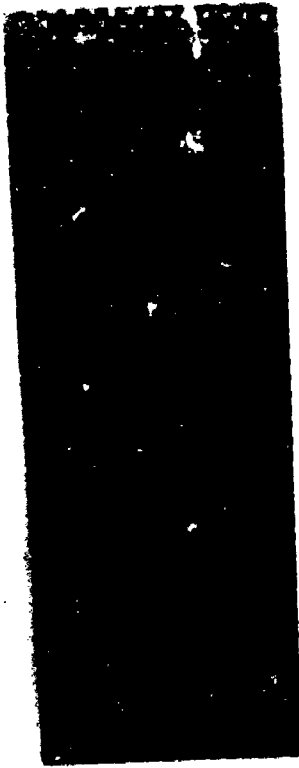
Figure 24. Longitudinal Crack in a Run-Out Specimen:
$S/\bar{X} = 0.70$, $\sigma_p/\bar{X} = 0.87$.

10-G-6   10-A-11

Figure 25.   Failure Modes at $S/\overline{X} = 0.8$ and $\sigma_p/\overline{X} = 0.95$:
N = 315,835 cycles for 10-G-6; $\sigma_p/\overline{X} = 0.87$:
N = 21,966 cycles for 10-A-11.

12-D-11   12-D-28
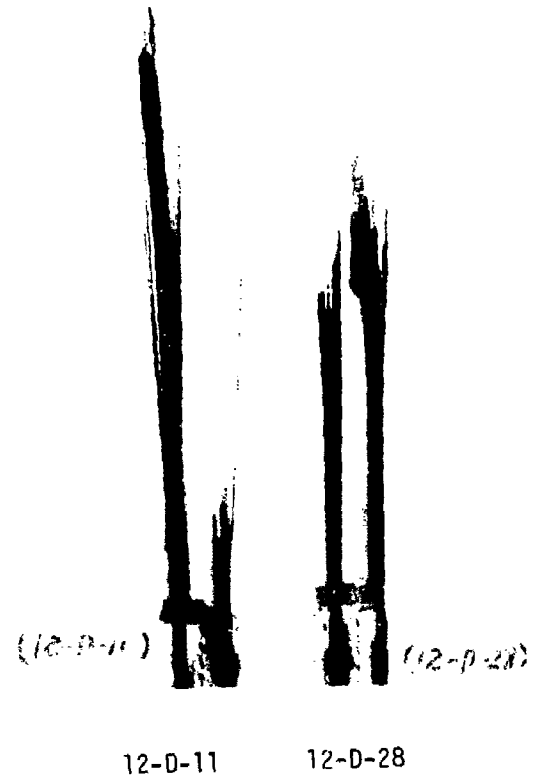
Figure 26.   Failure Modes at $S/\overline{X} = 0.87$:   N = 49,311 cycles for
12-D-11; N = 2,967 cycles for 12-D-28.

The fatigue stress of 0.925 $\overline{X}$ is perhaps too high to allow any static failure mode, Figure 20. At this stress level delamination occurs within a few hundred cycles, and hence all fatigue failures showed delamination.

As is clear by now, there is no monotonic change of the average failure mode with the fatigue stress. If the fatigue stress is either high (0.925 $\overline{X}$) or low (0.70 $\overline{X}$), much delamination occurs before the final failure. At the fatigue stresses between these two extremes, specimens can fail either before or after the development of full delamination. Early failures retain the typical static failure mode, and full delamination is observed only in those specimens with long lives.

7. EFFECT OF FAILURE ZONE ON STRENGTH AND LIFE

If many of the lower strengths or the shorter lives are the result of gripping, then a proper care should be exercised to minimize the effect of gripping. However, the use of glass/epoxy tabs seems sufficient to avoid any grip-related premature failures.

Figure 27 shows static strengths versus the corresponding failure zones for all four panels. Zone A is next to the upper grip of the MTS machine and zone E adjoins the moving, lower grip. No significant correlation can be drawn from the data in the figure.

A correlation between fatigue life and failure zone is shown in Figure 28 at each of the four fatigue stresses. Again, there does not appear to be any effect of gripping on the fatigue lives.

52
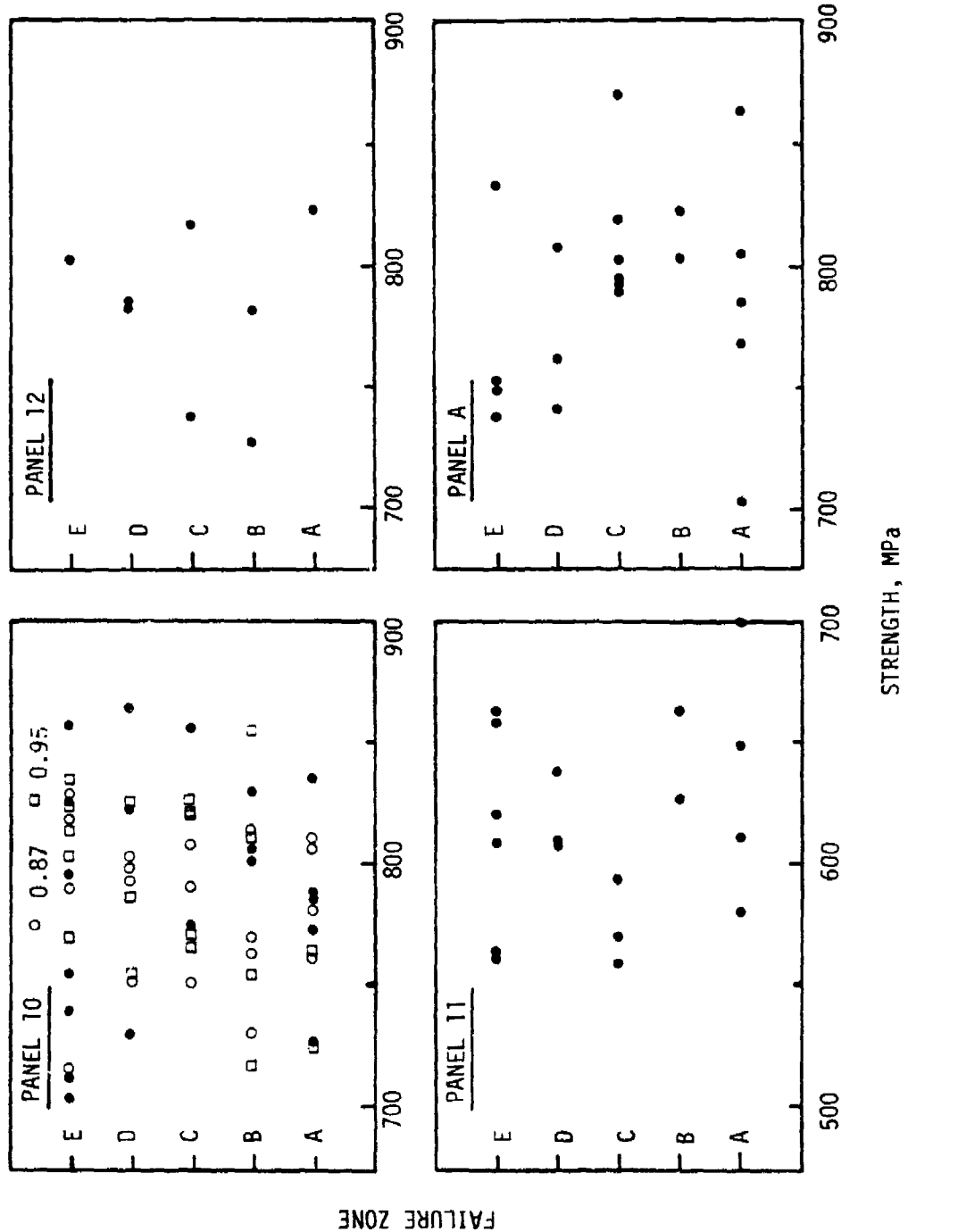
Figure 27. Correlations Between Strength and Failure Zone.
(Numbers indicate $\sigma_p/\overline{X}$.)
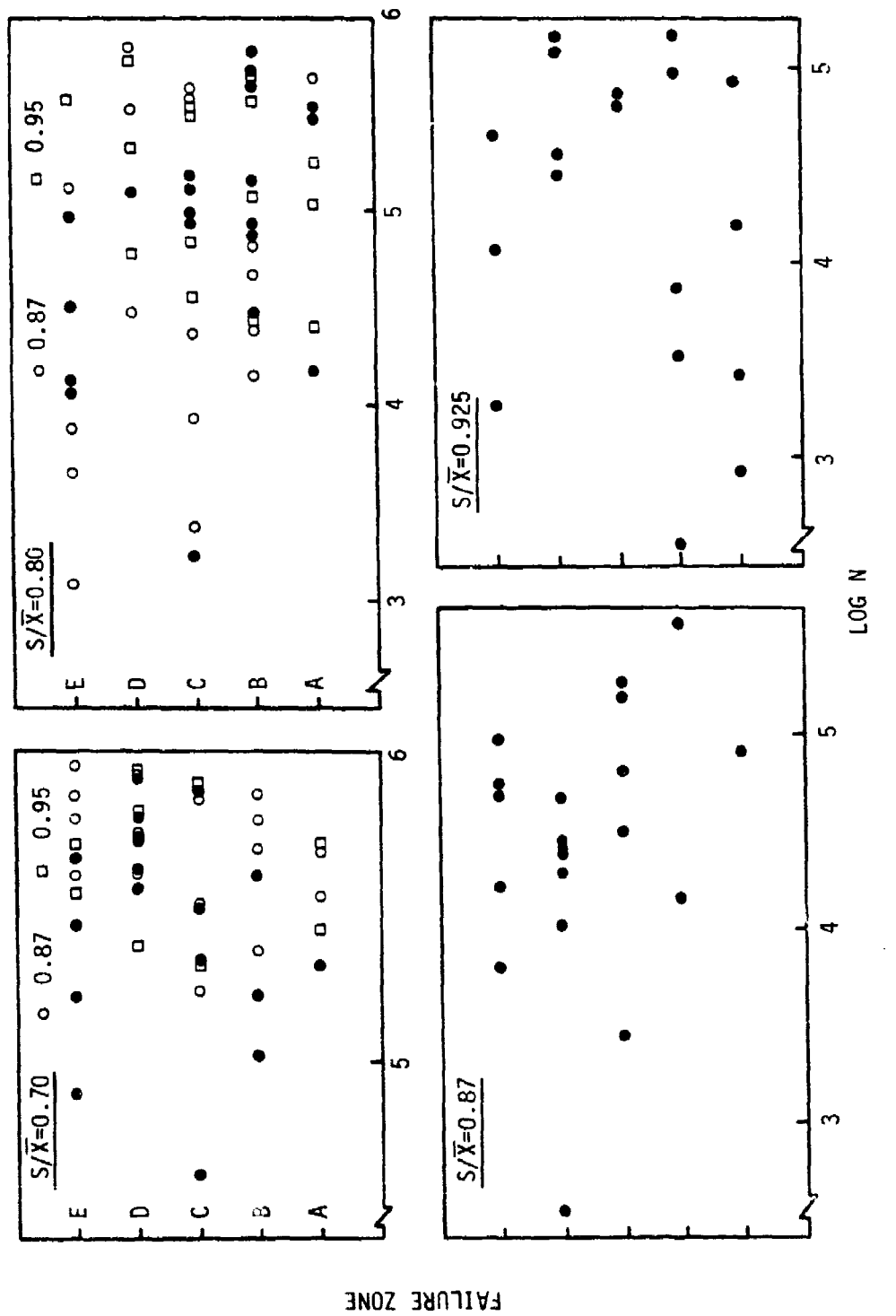
Figure 28. Correlations Between Life and Failure Zone.
(Numbers indicate $\sigma_p/\overline{X}$.)

8. FAILURE PROCESSES

The failure sequence of the present laminate has been found to be essentially the same as that of quasi-isotropic laminates [11-14]. That is, as the fatigue proceeds, cracks appear first in the 90-deg plies, next in the +45-deg plies, and finally in the -45-deg plies. As discussed earlier, delamination frequently preceded the final failure. In static tension, the sequence of ply failures was the same, but fewer cracks were observed. Also, delamination was rather limited.

The ply failures naturally depend on the residual stresses which are the result of anisotropic hygrothermal expansion behavior of unidirectional plies. Since swelling negates the curing strains at the room temperature, the moisture content must be determined to estimate the magnitude of the residual stresses. To this end, two specimens were dried in a vacuum oven at 70°C, and the results are shown in Figure 29. The moisture content in the laboratory environment is seen to be about 0.6%.

According to the classical laminate plated theory, the moisture content of 0.6% is not sufficient to render a graphite/epoxy laminate free of residual stresses [23]. However, it has been observed [14,24] that the first ply-failure stress is higher if the thickness of the lumped 90-deg plies is smaller. Also, there may be a stress relaxation resulting from a long storage of the panels since fabrication. In light of these contrasting observations, we assume the residual stresses to be negligible in the present laminates.

55
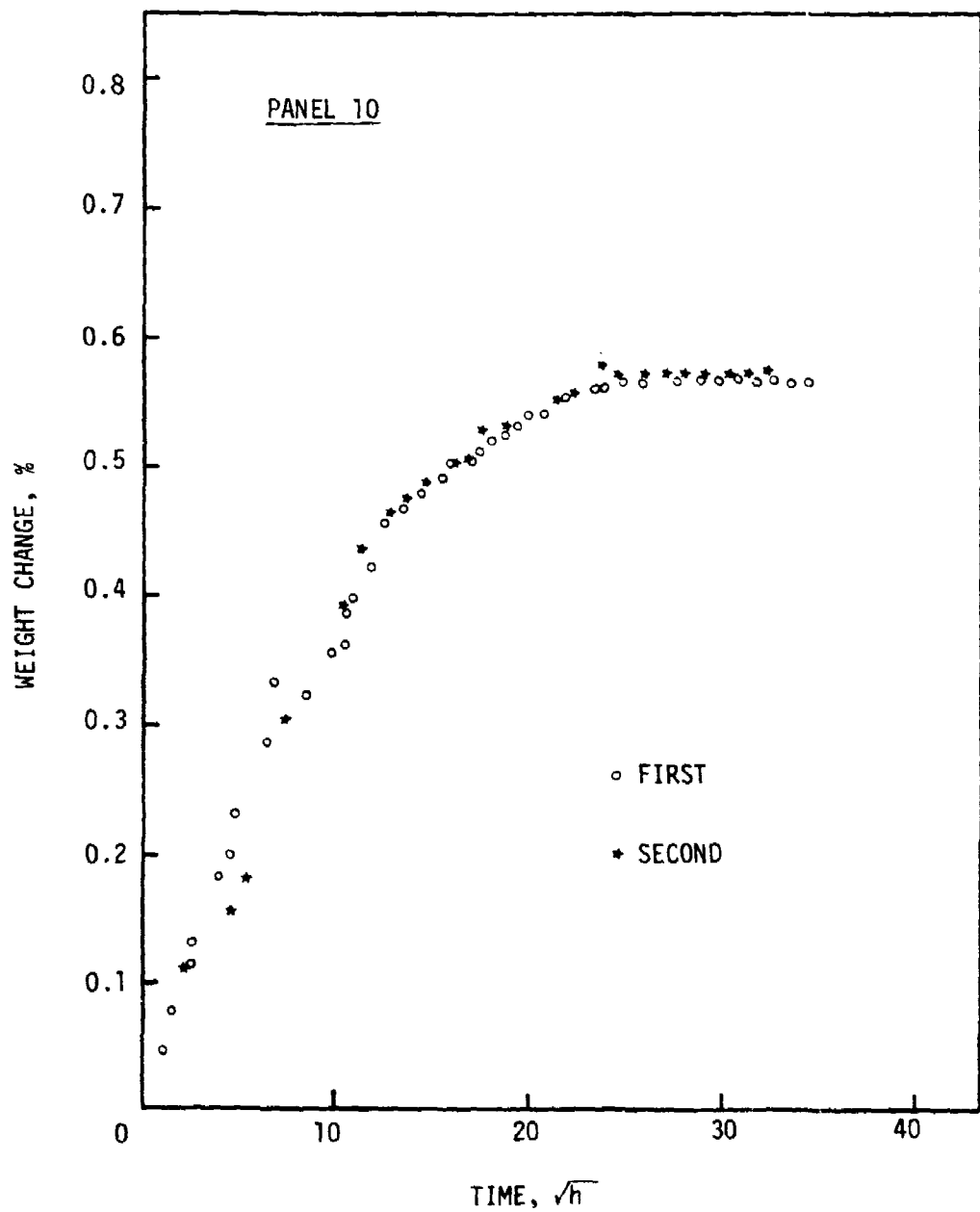
Figure 29.   Results of Moisture Desorption Tests.

56

Consequently, the first ply-failure strain of the laminates
will be almost equal to the transverse failure strain of unidirectional
lamina. Since the latter is found to be 7 mm/m from Reference [18] and
since the average failure strain of the laminates is about 11 mm/m,
the first ply-failure stress is estimated to be 7/11 $\overline{X}$ or 0.64 $\overline{X}$. In
reality, cracking of the 90-deg plies occurred between 0.70 $\overline{X}$ and
0.80 $\overline{X}$. At $\sigma_p/\overline{X}$ = 0.87 cracks were mostly confined in the 90-deg plies,
Figure 30. As the proof stress was raised to 0.95 $\overline{X}$, cracks appeared
in the $\pm$ 45-deg plies as well.

A typical fatigue failure observed at an edge is shown in
Figure 31. Notice the cracking of all constituent plies and
delaminations.

In general, delamination surfaces consisted of two distinct
areas: one shiny and the other dull, see Figure 16. SEM photographs
of a delamination surface between the 0-deg plies and 90-deg ply
are shown in Figure 32 at different magnifications. Close examinations
of those pictures reveal that the shiny area has bare fibers on the
surface, Figure 32(c), while the dull area only has traces of fibers
in the epoxy, Figure 32(d). Apparently, the bare fibers act like
convex mirrors, thereby producing a macroscopically shiny surface.
On the other hand, the fiber traces are similar to concave mirrors and
limit the reflection of light. Note that, at a magnification of 80x
on an SEM, there is no discernible difference between bare fibers and
fiber traces.

57

Figure 30. Cracks in the 90-deg Plies After Proof Test to 0.87 X.

Figure 31. Photomicrograph of a Polished Edge After Fatigue
at $S/\overline{X} = 0.925$.

Figure 32a. SEM Photograph of a Delamination Surface Between the 0-deg and 90-deg Plies. (Bare fibers are in the horizontal 0-deg plies.)
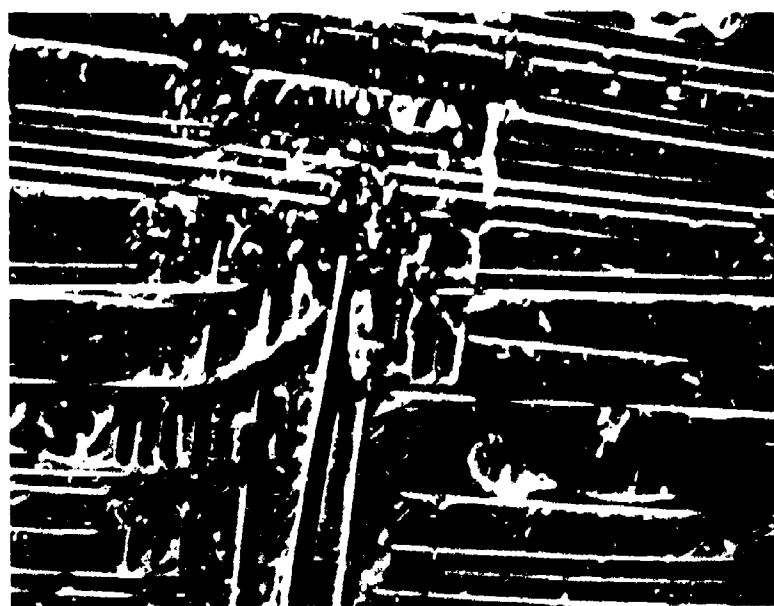
Figure 52b.   SEM Photograph Showing Both Bare Fibers and Fiber Traces.

Figure 32c. Magnified View of Bare Fibers.

62

Figure 32d. Magnified View of Fiber Traces.

Another observation to be made of Figure 32(a) is that almost no fibers in the 0-deg plies are broken at distances away from the final failure location. In the figure the horizontal fibers are in the 0-deg plies. Thus, the final failure seems to be the result of a localized fracture of the 0-deg plies.

9. EFFECT OF SPECIMEN WIDTH ON STRENGTH

In the earlier phase of the program, specimens were 25.4 mm wide. To study the possibility of adopting a reduced specimen width, we tested a few specimens which were only half as wide. Since the narrow specimens yielded higher strength, the nominal width of 12 mm was used in the subsequent tests.

Now at the end of the program we have much more extensive data on the strength of the narrow specimens. The final results are shown in Table 5.

For panels 11 and 12, the effect of specimen width on the average strength has been analyzed by using the Student t-test. It is concluded with 95% confidence that the average strength of the wide specimens is not as high as that of the narrow specimens for both panels.

TABLE 5

EFFECT OF SPECIMEN WIDTH

Panel No.	Specimen Width, mm	Average Strength, MPa	Coefficient of Variation, %	No. of Specimens	Is Difference Significant?
10	25.4	714.3		2	--
10	12.0	789.7	6.24	20	
11	25.4	557.7	6.11	6	Yes
11	12.0	609.1	7.23	20	
12	25.4	682.6[a]	6.20	12	Yes
12	12	782.0	3.46	8	

[a]Based on the average thickness measured on a microscope.

65

SECTION IV

SUMMARY AND CONCLUSIONS

The fatigue behavior of a $[0_2/90/\pm45]_s$ AS/3501-5A laminate
has been investigated through proof testing. The fatigue loading
was sinusoidal with the stress ratio of 0.1 and the frequency of
5 Hz. The proof stresses chosen were 0.87 $\overline{X}$ and 0.95 $\overline{X}$ where $\overline{X}$ is
the average static strength. In fatigue, an additional proof stress
was chosen: the maximum fatigue stress itself. The effect of proof
stress on life was studied at the fatigue stresses of 0.70 $\overline{X}$ and
0.80 $\overline{X}$. Additional fatigue tests were carried out at 0.60 $\overline{X}$,
0.87 $\overline{X}$ and 0.925 $\overline{X}$. The following conclusions can be drawn from
the present study.

1. The shape parameter for life distribution decreases with
increasing fatigue stress. The stress-logarithmic characteristic
life relation is quite linear down to 0.70 $\overline{X}$. All specimens tested
at 0.60 $\overline{X}$ survived 10^6 cycles.

2. The proof tests have little effect on both residual strength
and residual life after proof test. The residual strength and life
distributions are comparable to the respective initial distributions.

3. Strength-life relations were established at the fatigue
stresses of 0.70 $\overline{X}$ and 0.80 $\overline{X}$. These relations were verified by
proof testing. Thus, a minimum fatigue life can be assured by a
proof test.

4. A higher modulus is very likely to be an indication of a higher strength and a longer life. Since the modulus is rather related to the fiber volume content than to local defects, it is concluded that both strength and life depend on the fiber volume content more than anything else. Thus, the strength-life relationship seems to be via the fiber volume content.

5. Extensive delamination occurs before the final failure if the fatigue stress is too high, say 0.925 $\overline{X}$, or too low, say 0.70 $\overline{X}$. At a moderate fatigue stress of 0.80 $\overline{X}$, the amount of delamination increases with fatigue life: the transition from a static failure mode to a typical fatigue failure mode occurs around 20,000 cycles. Thus, the lack of delamination after the final failure can be taken as a sign of an early failure at the fatigue stress of 0.80 $\overline{X}$.

6. There is no correlation between the failure location and the corresponding strength and fatigue life. The effect of gripping is therefore negligible.

7. The failure processes in the present laminate are similar to those in quasi-isotropic laminates. The constituent plies fail in the following order: the 90-deg plies, the 45-deg plies, and the -45-deg plies. In static tension, delamination is negligible. However, the final fatigue failure is frequently preceded by extensive delamination. A delamination surface typically consists of two distinct areas: one shiny and the other dull. The shiny area has bare fibers on the surface while the dull area only has traces of fibers in the epoxy. Almost no fibers in the 0-deg plies are broken at distances away from the final

67

failure location. Therefore, the final failure seems to be the result of localized fracture of the 0-deg plies.

8. The narrow specimen width, 12 mm compared to 25.4 mm, results in a higher strength.

It cannot be overly emphasized that the foregoing conclusions are based only on the present study of a particular laminate. Some of these conclusions are in a slight contrast to the findings of other investigators on different laminates. The elucidation of reasons for such differences no doubt requires further effort in the area of fatigue behavior and proof testing of composite laminates.

REFERENCES

1. Haviland, R. P., Engineering Reliability and Long Life Design,
    D. Van Nostrand Co., New York, 1964.

2. Halpin, J. C., Jerina, K. L., and Johnson, T. A., "Characterization
    of Composites for the Purpose of Reliability Prediction",
    Analysis of Test Methods for High Modulus Fibers and Composites,
    ASTM STP 521, American Society for Testing and Materials, 1973,
    pp. 5-64.

3. Hahn, H. T. and Kim, R. Y., "Proof Testing of Composite Materials",
    J. Composite Materials, Vol. 9, 1975, pp. 297-311.

4. Awerbuch, J. and Hahn, H. T., "Fatigue and Proof-Testing of
    Unidirectional Graphite/Epoxy Composite", Fatigue of Filamentary
    Composite Materials, ASTM STP 636, American Society for Testing
    and Materials, 1977, pp. 248-266.

5. Yang, J. N. and Liu, M. D., "Residual Strength Degradation Model
    and Theory of Periodic Proof Tests for Graphite/Epoxy Laminates",
    J. Composite Materials, Vol. 11, 1977, pp. 176-203.

6. Wang, A. S. D., Chou, P. C., and Alper, J., "Effects of Proof-Test
    on the Strength and Fatigue Life of a Unidirectional Composite",
    AFML-TR-79-4189, May 1979.

7. Kim, R. Y. and Park, W. J., "Proof Testing Under Cyclic Tension-
    Tension Fatigue", J. Composite Materials, Vol. 14, 1980, pp. 69-79.

8. Hahn, H. T. and Tsai, S. W., "On the Behavior of Composite
    Laminates After Initial Failure", J. Composite Materials, Vol. 8,
    1974, pp. 288-305.

9. Tsai, S. W. and Hahn, H. T., "Failure Analysis of Composite
    Materials", Inelastic Behavior of Composite Materials, C. T. Herakovich,
    Ed., AMD-Vol. 13, ASME, 1975, pp. 73-96.

10. Broutman, L. J. and Sahu, S., "Progressive Damage of a Glass Reinforced
    Plastic During Fatigue", Proc. 24th SPI Conference, 1969, 11-D.

11. Hahn, H. T., "Fatigue Behavior and Life Prediction of Composite
    Laminates", AFML-TR-78-43, April 1978.

12. Reifsnider, K. L., Henneke, E. G., II and Stinchcomb, W. W.,
    "Defect-Property Relationships in Composite Materials", AFML-TR-76-81,
    April 1976; Part II, June 1977; Part III, June 1978; Part IV,
    June 1979.

13. Kim, R. Y. and Hahn, H. T., "Effect of Curing Stresses on the First Ply-Failure in Composite Laminates", J. Composite Materials, Vol. 13, 1979, pp. 2-16.

14. Kim, R. Y., "Experimental Assessment of Static and Fatigue Damage of Graphite/Epoxy Laminates", Advances in Materials, Proc. 3rd Int. Conf. on Composite Materials, Pergamon, 1980, pp. 1015-1028.

15. Guild, F. J., Walton, D., Adams, R. D., and Short, D., "The Application of Acoustic Emission to Fibre-Reinforced Composite Materials", Composites, Vol. 7, 1976, pp. 173-179.

16. Hahn, H. T., "Residual Stresses in Polymer Matrix Composite Laminates", J. Composite Materials, Vol. 10, 1976, pp. 266-278.

17. Hamstad, M. A., "Deformation and Failure Information from Composite Materials via Acoustic Emission", Preprint UCRL-81272, Lawrence Livermore Laboratory, November 1978.

18. Nguyen, N. Q. and Kardos, J. L., "Fatigue Failures of Composite Laminates", AFML-TR-79-4035, April 1979.

19. Cohen, A. C., "Maximum Likelihood Estimation in the Weibull Distribution Based on Complete and on Censored Samples", Technometrics, Vol. 7, 1965, pp. 579-588.

20. Whitney, J. M., "Fatigue Characterization of Composite Materials", AFML-TR-79-4111, October 1979.

21. Ryder, J. T. and Walker, E. K., "Ascertainment of the Effect of Compressive Loading on the Fatigue Lifetime of Graphite/Epoxy Laminates for Structural Applications", AFML-TR-76-241, December 1976.

22. Hahn, H. T. and Chiao, T. T., "Long-Term Behavior of Composite Materials", Advances in Composite Materials, Proc. 3rd Int. Conf. on Composite Materials, 1980, pp. 584-596.

23. Hahn, H. T. and Kim, R. Y., "Swelling of Composite Laminates", Advanced Composite Materials-Environmental Effects, ASTM STP 658, American Society for Testing and Materials, 1978, pp. 98-120.

24. Wang, A. S. D., "Growth Mechanisms of Transverse Cracks and Ply Delamination in Composite Laminates", Advances in Materials, Proc. 3rd Int. Conf. on Composite Materials, Pergamon, 1980, pp. 170-185.

APPENDIX A.   STATIC STRENGTHS

Panel 10

Specimen No.	Failure Zone	Static Strength, MPa	Ultimate Strain, mm/m	Modulus, GPa
10-A-2	B	829.16	12.58	60.81
10-A-3	C	856.74	11.44	74.39
10-A-4	E	712.78	10.22	70.46
10-A-5	E	826.27	11.34	70.74
10-A-6	D	824.41	12.16	68.95
10-B-1	A	835.09	12.42	65.43
10-B-2	B	802.76	11.08	76.12
10-B-3	B	806.41	10.64	69.71
10-B-4	E	857.57	11.94	66.12
10-B-5	A	788.48	10.54	69.22
10-B-7	E	704.99	9.50	61.43
10-B-8	A	726.09	10.54	64.05
10-B-9	E	754.84	10.76	69.77
10-B-10	D	730.57	10.20	68.88
10-B-11	D	864.53	11.16	75.43
10-B-21	C	775.80	11.20	69.29
10-B-22	E	796.48	12.10	65.64
10-B-23	A	787.38	11.60	67.91
10-B-24	A	773.18	11.30	68.40
10-E-2	E	739.95	11.72	64.40
Average $\overline{X}$		789.67	11.24	68.36
S. D.[a]		49.29	0.81	4.12
C. V.[b]		6.24%	7.21%	6.03%

[a] Standard deviation

[b] Coefficient of variation

71

Panel 11

Specimen No.	Failure Zone	Static Strength MPa	Ultimate Strain, mm/m	Modulus, GPa
11-B-2	D	638.44	-[a]	-
11-B-3	C	570.50	-[a]	-
11-B-4	A	580.61	-[a]	-
11-B-5	E	663.76	10.54	59.21
11-B-6	A	700.78	11.92	62.08
11-B-7	D	608.10	9.88	57.67
11-B-8	E	620.92	9.42	58.77
11-B-9	E	563.58	9.86	53.57
11-B-10	E	608.44	9.96	57.24
11-E-1	Tab	552.24	10.60	53.01
11-E-2	C	594.53	11.40	55.37
11-E-3	D	609.20	11.30	56.93
11-E-4	A	649.12	10.60	58.10
11-D-5	C	559.95	9.75	60.65
11-E-6	E	657.80	12.10	57.89
11-E-7	E	564.92	11.05	53.99
11-E-8	B	626.29	10.05	58.70
11-E-9	Tab	538.01	10.05	53.52
11-E-10	B	663.73	12.30	59.39
11-E-11	A	610.97	11.35	56.97
Average $\overline{X}$		609.09	10.71	57.23
S. D.		44.06	0.89	2.60
C. V.		7.23%	8.33%	4.54%

[a]Extensometer slipped

72

Panel 12

Specimen No.	Failure Zone	Static Strength, MPa	Ultimate Strain, mm/m	Modulus, GPa
12-D-1	D	783.99	11.4	69.16
12-D-2	C	816.17	11.9	68.63
12-D-3	C	738.90	11.2	66.61
12-D-4	D	784.55	11.5	68.65
12-D-5	E	802.41	11.4	71.02
12-D-6	B	779.87	11.4	68.80
12-D-7	A	822.42	11.3	72.7?
12-D-8	B	727.36	10.5	69.89
Average $\overline{X}$		781.96	11.3	69.44
S. D.		33.96	0.4	1.83
C. V.		4.34%	3.46%	2.64%

Panel A

Specimen No.	Failure Zone	Static Strength, MPa	Ultimate Strain, mm/m	Modulus, GPa
A-a-1	C	793.16	11.32	70.06
A-a-2	D	741.09	10.98	67.49
A-a-3	C	819.28	11.34	72.25
A-a-4	A	768.74	11.29	68.11
A-a-5	D	807.34	10.70	75.48
A-a-6	E	749.29	10.74	69.77
A-a-7	E	739.80	11.74	63.02
A-a-8	A	805.95	11.26	71.57
A-a-9	B	823.03	11.54	71.32
A-a-10	C	802.40	12.64	63.48
A-a-11	E	754.06	11.76	64.12
A-a-12	A	838.22	12.10	69.27
A-a-13	A	785.08	10.86	72.29
A-a-14	D	737.57	10.54	70.02
A-a-15	B	803.58	11.32	70.99
A-a-16	C	870.68	12.31	70.71
A-a-17	A	703.66	10.31	68.25
A-a-18	C	794.88	11.54	68.91
A-a-19	E	833.60	11.50	72.48
A-a-20	C	790.50	10.51	75.21
Average $\overline{X}$		788.11	11.32	69.74
S. D.		41.06	0.61	3.39
C. V.		5.21%	5.43%	4.86%

APPENDIX B.   FATIGUE LIVES

Panel 11

$S/\overline{X} = 0.70$, $\sigma_p/\overline{X} = 0.70$

Specimen No.	Failure Zone	Fatigue Cycles N	Modulus, GPa
11-E-13	D	518,245	58.86
11-E-14	E	166,105	54.94
11-E-15	C	768,851	59.53
11-E-16	D	548,730	58.92
11-E-17	C	314,101	57.46
11-E-18	A	208,910	53.57
11-E-19	E	280,803	54.25
11-E-20	B	107,387	57.46
11-A-11	C	43,490	51.00
11-A-12	C	215,973	54.39
11-C-1	B	404,999	55.52
11-C-2	-[a]	1,000,000	60.32
11-C-3	D	428,489	58.41
11-C-4	B	166,736	54.24
11-C-5	E	80,341	53.10
11-C-6	D	362,138	56.70
11-C-7	E	463,126	58.05
11-D-6	D	623,387	57.15
11-D-7	-[a]	1,000,000	58.96
11-D-8	D	843,210	57.61

[a]Run-out

75

Panel 10

$S/\overline{X} = 0.8^\wedge$, $\sigma_p/\overline{X} = 0.80$

Specimen No.	Failure Zone	Fatigue Cycles N	Modulus, GPa
10-E-19	B	154,852	69.57
10-E-20	B	427,694	69.16
10-E-21	B	544,957	70.65
10-E-22	E	15,164	64.95
10-E-24	C	131,866	67.73
10-F-1	B	77,264	65.84
10-F-2	B	158,276	68.33
10-F-3	B	31,756	65.80
10-F-4	C	87,562	66.28
10-F-5	C	1,806	64.05
10-F-6	E	33,601	66.24
10-F-7	A	17,538	64.83
10-F-8	E	95,950	66.34
10-F-9	B	686,010	71.85
10-F-10	D	131,684	67.64
10-F-11	A	319,141	69.73
10-F-12	E	12,487	64.20
10-F-13	C	95.396	66.11
10-F-14	A	369,537	70.00
10-F-15	C	158,821	69.11

Panel 12

$S/\overline{X} = 0.87$, $\sigma_p/\overline{X} = 0.87$

Specimen No.	Failure Zone	Fatigue Cycles N	Modulus, GPa
12-D-9	B	40,031	69.55
12-D-10	C	64,168	69.79
12-D-11	D	49,311	69.13
12-D-12	C	196,202	72.95
12-D-13	C	167,924	72.22
12-D-14	A	80,343	70.76
12-D-15	D	46,792	69.54
12-D-16	E	17,854	64.85
12-D-17	E	54,852	70.15
12-D-18	C	31,420	70.05
12-D-19	D	10,252	66.80
12-D-20	B	380,722	74.18
12-D-21	E	98,712	72.06
12-D-22	D	350	64.83
12-D-23	D	19,252	67.97
12-D-24	E	6,033	65.92
12-D-25	D	25,218	66.30
12-D-26	D	24,794	67.85
12-D-27	D	28,647	68.71
12-D-28	C	2,967	65.16

Panel A

$S/\overline{X} = 0.925$, $\sigma_p/\overline{X} = 0.925$

Specimen No.	Failure Zone	Fatigue Cycles N	Modulus, GPa
A-a-21	C	74,501	72.43
A-a-22	A	15,711	70.94
A-a-23	D	162,317	75.15
A-a-24	B	7,428	68.51
A-a-25	B	98,731	73.00
A-a-26	A	84,056	72.26
A-a-27	E	11,347	69.53
A-a-28	E	1,979	65.67
A-a-29	A	_a	64.20
A-a-30	A	2,826	66.51
A-a-31	C	64,847	72.19
A-a-32	B	350	65.33
A-a-33	A	_a	71.06
A-a-34	E	47,165	71.71
A-a-35	D	37,112	71.47
A-a-36	D	126,091	73.26
A-a-37	A	854	65.68
A-a-38	D	29,709	70.91
A-a-39	B	148,573	72.80
A-a-40	B	3,346	67.13

[a]Failure during proof test

APPENDIX C.   STRENGTHS AFTER PROOF TEST

Panel 10

$\sigma_p/\overline{X} = 0.87$

Specimen No.	Failure Zone	Residual Strength MPa
10-B-23	E	716.37
10-B-17	B	730.17
10-C-8	C	751.74
10-C-6	D	753.73
10-E-15	A	761.94
10-C-1	B	764.42
10-B-21	B	769.66
10-C-4	A	782.28
10-C-12	E	789.86
10-C-5	C	790.90
10-B-16	D	793.17
10-C-11	D	798.21
10-E-16	D	803.58
10-C-9	A	806.48
10-C-3	C	808.20
10-B15	A	811.24
10-C-7	B	814.41
10-E-14	E	818.34
10-C-2	E	827.03
10-B-18	Tab	845.16

Panel 10

$\sigma_p/\overline{X} = 0.95$

Specimen No.	Failure Zone	Residual Strength MPa
10-D-11	D	754.56
10-E-11	B	755.73
10-D-10	A	764.28
10-D-16	C	766.70
10-D-12	E	769.45
10-E-6	C	772.21
10-E-7	D	786.69
10-E-13	E	803.17
10-D-5	Tab	812.82
10-D-18	B	813.24
10-E-12	E	814.41
10-D-6	C	819.03
10-D-15	C	821.37
10-D-19	C	821.86
10-D-14	E	823.78
10-D-13	D	823.99
10-D-17	E	835.30
10-D-7	B	855.29

APPENDIX D. FATIGUE LIVES AFTER PROOF TEST

Panel 11

$S/\overline{X} = 0.70$, $\sigma_p/\overline{X} = 0.87$

Specimen No.	Failure Zone	Fatigue Cycles N	Modulus, GPa
11-C-11	D	841,398	56.96
11-C-12	_a	1,000,000	59.72
11-C-13	C	717,752	56.30
11-C-14	E	752,264	50.77
11-C-15	B	735,134	58.00
11-C-16	A	483,396	54.95
11-C-17	E	409,216	55.49
11-C-18	B	498,211	55.75
11-C-19	C	327,678	53.81
11-C-20	_a	1,000,000	57.65
11-C-21	A	341,233	54.70
11-C-22	B	607,508	55.86
11-D-1	E	614,414	57.10
11-D-2	_a	1,000,000	61.76
11-D-3	Tab	_b	51.31
11-D-4	C	173,427	52.91
11-D-5	B	231,216	55.68
11-C-8	D	558,962	55.65
11-F-4	D	428,910	55.18
11-F-5	E	923,671	57.63

[a] Run-out

[b] Failure during proof test

Panel 11

$S/\overline{X} = 0.70$, $\sigma_p/\overline{X} = 0.95$

Specimen No.	Failure Zone	Fatigue Cycles N	Modulus GPa
11-D-9	E	511,179	57.25[c]
11-D-10	D	904,845	
11-D-11	A	271,562	54.26
11-D-12	D	247,880	54.85
11-D-13	-[a]	1,000,000	58.77
11-D-14	D	-[b]	54.22
11-D-15	C	211,287	53.32
11-D-16	A	510,605	57.14
11-D-17	-[a]	1,000,000	59.46
11-D-18	E	365,371	56.25
11-D-19	E	-[b]	51.55
11-D-20	C	811,423	58.61
11-D-21	B	-[b]	52.19
11-D-22	-[a]	1,000,000	58.48
11-D-26	-[a]	1,000,000	58.70
11-D-27	D	663,092	57.66
11-D-28	D	-[b]	51.83
11-F-1	-[a]	1,000,000	60.34
11-F-2	Tab	-[b]	52.34
11-F-3	E	448,621	56.42

[a]Run-out

[b]Failure during proof test

[c]Extensometer slipped

Panel 10

$$S/\overline{X} = 0.80, \; \sigma_p/\overline{X} = 0.87$$

Specimen No.	Failure Zone	Fatigue Cycles N	Modulus, GPa
10-F-16	Tab	12,656	65.65
10-F-17	E	146,895	69.82
10-F-18	E	7,775	64.96
10-F-19	A	511,676	71.49
10-F-20	B	16,859	66.80
10-F-21	D	352,311	69.96
10-F-22	C	382,078	71.16
10-F-23	C	_a	62.20
10-F-24	E	12,045	65.76
10-F-25	E	4,784	63.79
10-G-1	D	712,211	72.24
10-G-2	D	32,734	67.82
10-G-3	B	67,993	68.96
10-G-4	C	421,184	70.55
10-A-11	C	21,966	67.45
10-A-12	B	26,983	68.89
10-A-13	B	48,856	68.14
10-A-14	C	98,703	69.12
10-A-15	C	8,509	64.31
10-A-16	C	370,174	70.25
10-A-17	B	164,644	68.18

[a]Failure during proof test

Panel 10

$S/\overline{X} = 0.80$, $\sigma_p/\overline{X} = 0.95$

Specimen No.	Failure Zone	Fatigue Cycles N	Modulus GPa
10-G-5	B	389,428	68.57
10-G-6	C	315,835	67.71
10-G-7	E	$-^a$	66.30
10-G-8	C	69,413	65.57
10-G-9	C	37,071	65.80
10-G-10	A	197,566	66.98
10-G-11	B	$-^a$	64.13
10-G-12	B	120,159	64.33
10-G-13	B	29,936	64.95
10-G-14	C	339,657	73.02
10-G-15	A	117,738	66.10
10-G-16	D	62,870	66.15
10-G-17	C	$-^a$	60.37
10-G-18	B	$-^a$	$-^b$
10-H-5	D	211,033	67.46
10-H-6	B	512,130	70.65
10-H-7	D	633,226	70.00
10-G-19	E	459,980	69.45
10-G-20	A	27,740	63.78
10-G-21	D	$-^a$	63.38

[a]Failure during proof test

[b]Extensometer slipped

84